Paleoceanography and Paleoclimatology

RESEARCH ARTICLE
10.1029/2018PA003338

Key Points:
- During the Aptian, episodes of anoxia/euxinia developed in the South Atlantic with strong cyclicity
- Hydrographic restriction of the northern South Atlantic during the Aptian preconditioned the basin for anoxic episodes
- Astronomically driven changes in terrestrial runoff led to episodic stratification of the basin and development of anoxia/euxinia

Supporting Information:
- Supporting Information S1
- Table S1

Correspondence to:
L. Behrooz,
lb13902@bristol.ac.uk

Citation:
Behrooz, L., Naafs, B. D. A., Dickson, A. J., Love, G. D., Batenburg, S. J., & Pancost, R. D. (2018). Astronomically driven variations in depositional environments in the South Atlantic during the Early Cretaceous. *Paleoceanography and Paleoclimatology*, *33*, 894–912. https://doi.org/10.1029/2018PA003338

Received 7 FEB 2018
Accepted 23 JUL 2018
Accepted article online 1 AUG 2018
Published online 25 AUG 2018

Astronomically Driven Variations in Depositional Environments in the South Atlantic During the Early Cretaceous

L. Behrooz[1,2], B. D. A. Naafs[1,2], A. J. Dickson[4,5], G. D. Love[6], S. J. Batenburg[4], and R. D. Pancost[1,2,3]

[1]Organic Geochemistry Unit, School of Chemistry, University of Bristol, Bristol, UK, [2]Cabot Institute, University of Bristol, Bristol, UK, [3]School of Earth Science, University of Bristol, Bristol, UK, [4]Department of Earth Sciences, University of Oxford, Oxford, UK, [5]Now at Department of Earth Sciences, Royal Holloway University of London, London, UK, [6]Department of Earth Sciences, University of California, Riverside, CA, USA

Abstract The extent and persistence of anoxia in the South Atlantic Ocean during its early opening phase in the Early Cretaceous is not well constrained, hindering a holistic understanding of the processes and mechanisms that drive past changes in water column redox conditions, as well as the impacts of such changes on marine ecosystems. Here we provide high-resolution geochemical records from Deep Sea Drilling Project Site 364 that document variations in redox conditions, chemocline depth, marine productivity, and marine ecosystem dynamics in the northern South Atlantic during the Aptian. We show that many of these parameters varied across discrete sedimentary cycles expressed in the Deep Sea Drilling Project 364 succession. Our data indicate that during the initial stages of basin development, anoxic and euxinic conditions were prevalent and occasionally extended into the upper water column. However, strong cyclicity in sedimentological and geochemical parameters imply that the anoxia/euxinia was not a persistent state. We argue that the water column redox conditions during the Aptian were driven by changes in the hydrological cycle, induced by variations in astronomical forcing. We suggest that the episodically amplified hydrological cycle not only enhanced nutrient availability and marine productivity, but might also have caused density-driven upper ocean stratification. The presence of black shales of similar age in other ocean basins suggests that this mechanism is broadly important for the formation of Early Cretaceous organic-rich successions.

1. Introduction

The Cretaceous Period (~145–66 Ma) was characterized by a greenhouse climate (Hay, 2008, and references therein), with elevated atmospheric CO_2 levels (e.g., Foster et al., 2017; Naafs et al., 2016), high sea surface temperatures (e.g., Bice et al., 2006; Naafs & Pancost, 2016; O'Brien et al., 2017; Schouten et al., 2003), and little or no continental ice (Huber et al., 2002; MacLeod et al., 2013). Superimposed on this general greenhouse climate are the oceanic anoxic events (OAEs). Classically, OAEs are time intervals associated with expansion of anoxia and deposition of organic-rich black shales in the ocean (Jenkyns, 2010, and references therein), although some OAEs have also been identified in lake sediments (Xu et al., 2017). OAEs are associated with intense perturbations in global climate, ocean chemistry, and global biogeochemical cycles (Jenkyns, 2010), reflected, for example, in the carbon isotope excursions (CIEs) that accompany the major OAEs. Some OAEs have been associated with a positive CIE (e.g., OAE 2) and others with a negative CIE (Toarcian OAE), and some, like OAE 1a, contain both (see review by Jenkyns, 2010).

The occurrence of anoxia during the Cretaceous, however, was not exclusive to OAEs, as black shales formed at more limited regional scales at other times (e.g., C. Huang et al., 2010). The regional formation of black shales is dominated by local factors, for example, changes in nutrient availability, hydrology and water column stratification, and basin morphology. Preservation of organic-rich sediments is frequently linked to the development of anoxia, induced by either increased primary productivity and organic matter (OM) export overwhelming the rate of OM remineralization and/or decreased oxygen flux resulting in decreased OM remineralization. Black shales can occur as both singular sedimentary units or as repetitive units interbedded with organic-lean facies (Beckmann et al., 2005; Hofmann & Wagner, 2011; C. Huang et al., 2010; Kuypers et al., 2004; Malinverno et al., 2010; Meyers et al., 2006; Wagner et al., 2004), the latter of which is often attributed

to climate variability driven by astronomical forcing during the Cretaceous. Identifying the factors involved in the formation of Cretaceous black shales can provide a better understanding of Cretaceous biogeochemical cycles and climate feedbacks, as well as the formation of hydrocarbon source rocks.

Within the Cretaceous, the Aptian Stage is of particular interest as the opening of the South Atlantic started during this time period, leading to the development of a series of local rift basins in the southern and equatorial South Atlantic that were potentially prone to the development of black shales (e.g., Pérez-Díaz & Eagles, 2017). In addition, one of the major OAEs occurred during the Aptian: OAE 1a (Bralower et al., 1994). Therefore, there is much interest in the Aptian carbon cycle on both short (e.g., C. Huang et al., 2010) and long timescales (Bralower et al., 1994; Jenkyns et al., 2012). However, to the best of our knowledge there are remarkably few studies on Aptian organic carbon production and preservation from the South Atlantic (Bralower et al., 1994; Foresman, 1984; Jenkyns et al., 2012; Naafs & Pancost, 2014; Raynaud & Robert, 1978; Simoneit, 1978; Stein et al., 1986; Zimmerman et al., 1987) or even the Southern Hemisphere (van Breugel et al., 2007), and most of these are of low stratigraphic resolution. Almost all orbitally resolved records (i.e., with sampling steps at $<$~10–20-kyr intervals) from this period are from Europe (e.g., C. Huang et al., 2010). Early ocean drilling expeditions (e.g., Leg 40 Shipboard Scientific Party, 1978) recovered Aptian black shales in the northern South Atlantic and described the organic-rich to organic-lean interchanging nature of these successions. However, the triggering factors involved in the formation of these organic-rich layers and their alternating nature are not fully constrained. Here we provide high-resolution records of total organic carbon (TOC), total sulfur, and carbonate (%$CaCO_3$) contents to trace astronomically paced variations in the depositional environment of the northern South Atlantic (Site 364, at ~25°S paleolatitude) during the Aptian. In addition, high-resolution molecular organic geochemical analyses are provided from selected intervals to test whether apparently astronomically forced variations in sedimentary facies are related to primary marine productivity, chemocline expansion, or marine anoxia.

2. Samples and Methods

2.1. Sampling Location and Lithology

Deep Sea Drilling Project (DSDP) Leg 40, Site 364 (modern latitude: 11°34.32′S, 11°58.30′E, 2,450 m water depth), is located in the Kwanza Basin of the South Atlantic (Leg 40 Shipboard Scientific Party, 1978) and was drilled on the seaward edge of the salt plateau at the transition from the outer Kwanza Basin to the Benguela Basin (Leg 40 Shipboard Scientific Party, 1978). Site 364 covers a 427-m cored section (46 cores) to a bottom depth of 1,086 m below sea floor (bsf; top of the Aptian evaporite and salt formations) and consists of sediments that are Pleistocene to Early Cretaceous in age (Kochhann et al., 2014; Leg 40 Shipboard Scientific Party, 1978).

Site 364 is divided into seven lithological units (e.g., Leg 40 Shipboard Scientific Party, 1978; R. Matsumoto et al., 1978), with Units 6 and 7 investigated here. Unit 6 is predominantly composed of calcium carbonate (limestone), with a TOC content $<$3 wt %. The underlying Unit 7, the deepest lithological section of Site 364, comprises dolomitic limestones and thin black shales, with TOC contents as high as 40 wt % (Leg 40 Shipboard Scientific Party, 1978; T. Matsumoto, 1978; Raynaud & Robert, 1978; Simoneit, 1978). On the basis of the proportion of black shales, Unit 7 is divided into two subunits: 7a (Cores 39 to 41) with fewer and 7b (Cores 42 to 46) with more abundant and more intense black shale horizons (Leg 40 Shipboard Scientific Party, 1978). Guided by previous work (Leg 40 Shipboard Scientific Party, 1978; Naafs & Pancost, 2014), we mainly focus on subunit 7b (1,020–1,086 m bsf), characterized by the highest TOC contents and apparent pronounced cyclic variation in lithology. The timing of deposition of Unit 7 (Aptian) and Unit 6 (Aptian–Late Aptian) coincided with the initial opening of the South Atlantic and deepening of the basin (Zimmerman et al., 1987). During this time DSDP Site 364 was located at approximately 25°S, 10°W paleolatitude. Biostratigraphic evidence indicates that sediments at Site 364 were deposited on a continental shelf setting (Kochhann et al., 2014). The paleodepth of Site 364 during the Early Cretaceous (Unit 7) is estimated to be ~300–400 m (Zimmerman et al., 1987).

2.2. Analytical Methods

A total of 288 samples was obtained from the International Ocean Discovery Programme Bremen Core Repository, Germany. Unit 7b was sampled with a resolution of approximately 10 cm (250 samples). Thirty-

four samples were taken from Unit 7a and Unit 6 at a lower resolution. Bulk samples were freeze dried to remove excess water and were powdered using either a ball mill device or a mortar and pestle.

2.2.1. Bulk Geochemistry

Total carbon (C) and inorganic carbon (IC) contents were determined using a CHN elemental analyzer Eurovector EA 3000 and Strohlein Coulomat 702, respectively. All elemental analyses were performed in duplicate, and the presented data reflect the mean of these duplicates. TOC was determined by C and IC differences. To analyze bulk organic stable carbon isotopic ratios ($\delta^{13}C_{org}$), IC was removed using 2 M HCl acid. Sample tubes were placed in a water bath and heated at ~60 to 80 °C for 5 hr to aid the reaction (also ensuring the removal of pyrite). Samples were then repowdered and dried in an oven at 50 °C for 24 hr. Between 10 and 25 μg of each sample (depending on TOC content) were used to measure $\delta^{13}C_{org}$ at the Open University, UK. $\delta^{13}C_{org}$ was measured using a Thermo Flash HT Elemental Analyzer coupled to a Thermo Finnegan MAT 253 mass spectrometer (with the 1 σ uncertainty of 0.03‰, 0.09‰, and 0.01‰ for IAEA CH-6, NIST 8573, and IR-R041 standards, respectively; $n = 20$).

A selection of 68 samples from Unit 7b with an average resolution of ~50 cm were selected for Rock-Eval analyses. Rock-Eval analyses were performed using a Rock-Eval 6 instrument to obtain estimates of the hydrogen index (HI) and the temperature of maximum hydrocarbon generation (T_{max}). Respective 2σ uncertainties were estimated with repeated measurements of an in-house shale standard (St. Audries Bay Shale) and were 3 mg HC/g TOC and 19 °C. Approximately 30–50 mg of dried sample powders was weighed for each measurement.

2.2.2. Biomarker Extraction

The same 68 samples used to obtain Rock-Eval data from Unit 7b, alongside 14 samples from Unit 7a and 20 samples from Unit 6, were selected for detailed biomarker analysis. To obtain total lipid extracts (TLEs), 14 g of each sample was extracted with 20 ml of dichloromethane (DCM):methanol (MeOH; 9:1, vol) by microwave-assisted method (MILESTONIE Ethos Ex Microwave solvent extraction). The microwave program consisted of a 10-min ramp to 70 °C (maximum 1,000 W), followed by a 10-min hold at 70 °C (maximum 1,000 W), and a 20-min cooling period. Activated copper turnings were added to the TLEs for 24 hr to remove elemental sulfur. The TLE was then concentrated using rotatory evaporator and separated into three fractions (aliphatic, aromatic, and polar) using short (4-cm) silica gel open column chromatography. Aliphatic, aromatic, and polar fractions were eluted using 3 ml of hexane, 4 ml of hexane:DCM (3:1), and 4 ml of DCM:MeOH (1:2), respectively. All fractions were then dried under a gentle stream of N_2. To quantify the abundance of aromatic biomarkers, 1.25 μg of C_{36} *n*-alkane was added as an internal standard to the aromatic fractions. We did not determine exact response factors for the aromatic biomarkers, and the quantifications should thus be considered as semiquantitative.

Incorporation of inorganic sulfur into unsaturated bonds of hydrocarbons within the water column or sediment results in the formation of sulfurized hydrocarbon moieties in the polar fraction (Sinninghe Damsté & de Leeuw, 1990), potentially biasing the biomarker results if only the aliphatic and aromatic fractions are analyzed. To explore some aspects of the sulfurized biomarker assemblage, the polar fraction of one black shale sample from Unit 7b was desulfurized using Raney Nickel desulfurization and subsequent hydrogenation (Sinninghe Damsté et al., 1989).

2.2.3. Biomarker Analysis

Biomarker distributions in the aliphatic, aromatic, and desulfurized polar fractions were analyzed using a Thermo Scientific™ ISQ Series Single Quadruple gas chromatography-mass spectrometry (GC-MS) system. Separation of compounds was performed on a Zebron nonpolar column (50 m × 0.32 mm, 0.10-μm film thickness). The injection volume was 1 μl. The GC programme was injection at 70 °C (1-min hold), heating to 130 °C at a rate of 20 °C/min, then to 300 °C at 4 °C/min, followed by a 24-min hold. The mass spectrometer continuously scanned between *m/z* 50 and 650. Identification of biomarkers was carried out based on published retention times and spectra as well as comparison with standard samples.

In addition to the classical GC-MS system, 27 samples from Core 43 were analyzed using metastable reaction monitoring-GC-MS (MRM-GC-MS) conducted at University of California Riverside, United States, to identify and quantify isomers of methylsteranes and methylhopanes. The MRM-GC-MS system operates on a Waters AutoSpec Premier mass spectrometer equipped with a HP 6890 gas chromatograph and DB-1MS coated capillary column (60 m × 0.25 mm, 0.25-μm film thickness) using He as carrier gas. The GC

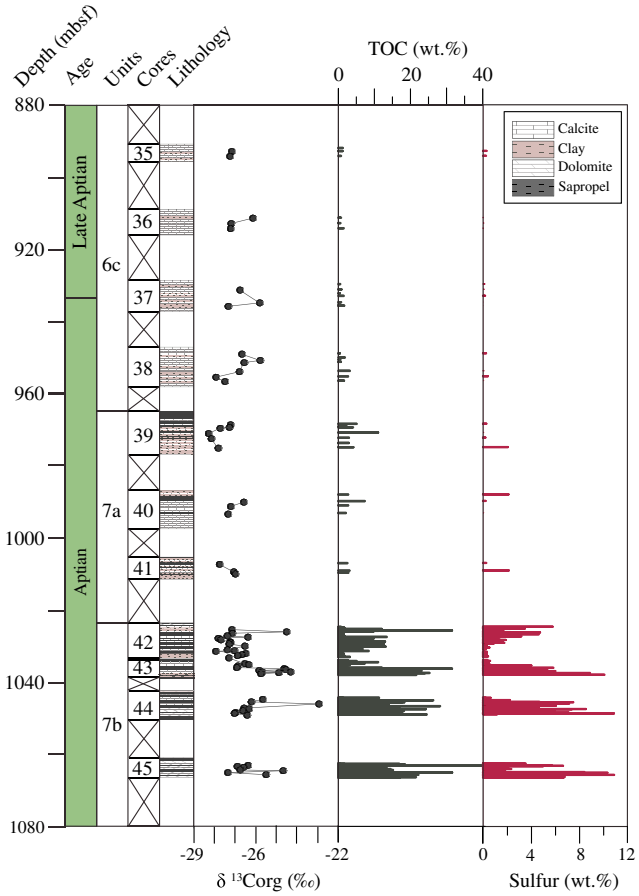

Figure 1. Lithology (Leg 40 Shipboard Scientific Party, 1978), bulk $\delta^{13}C_{org}$, total organic carbon (TOC) content, and sulfur content across Units 7b, 7a, and 6 (1,070–890 m below sea floor [bsf]) for Deep Sea Drilling Project Site 364. Note the presence of multiple core gaps.

temperature program consisted of an initial hold at 60 °C for 2 min, heating to 150 °C at 10 °C/min, followed by heating to 320 °C at 3 °C/min, and a final hold for 22 min. Analyses were performed via splitless injection at 320 °C in electron impact mode, with an ionization energy of 70 eV and an accelerating voltage of 8 kV. MRM transitions for C_{27}–C_{35} hopanes, C_{31}–C_{36} methylhopanes, C_{21}–C_{22} and C_{26}–C_{30} regular (4-desmethyl) steranes, C_{30} methylsteranes, and C_{19}–C_{26} tricyclics were monitored. Polycyclic biomarker alkanes (tricyclic terpanes, hopanes, steranes, etc.) were quantified by addition of a deuterated C_{29} sterane standard [d4-ααα-24-ethylcholestane (20R)] to aliphatic hydrocarbon fractions and comparison of relative peak areas.

Compound-specific $\delta^{13}C$ of the saturated hydrocarbon fraction was determined for two samples (one carbonate and one black shale) to explore the source of the biomarker 2,6,10,15,19-pentamethylicosane (PMI; e.g., Pancost et al., 2000). For this purpose, we used an Agilent Industries 7890A gas chromatograph coupled to an IsoPrime 100 GC-combustion-isotope ratio MS system. Samples were introduced onto a capillary column (50 m × 0.32 m, 0.17 μm film thickness) using He for carrier gas. The GC oven temperature programme was the same as for GC-MS analyses. Samples were measured in duplicate, and the presented value reflects the mean of duplicates. The $\delta^{13}C$ values were converted to Vienna Peedee Belemnite by bracketing with an in-house gas (CO_2) of known $\delta^{13}C$ value. Instrument stability was monitored by regular analysis of an in-house fatty acid methyl ester standard mixture; long-term precision is ±0.3‰.

2.3. Time Series Analyses

Time series analyses were performed on the whole TOC data set of Unit 7b (Cores 42–45) and on the upper interval from 1,024.62 to 1,037.92 m bsf (Cores 42 and 43). Power spectra were generated with Redfit 3.8 (Schulz & Mudelsee, 2002), using a Welch window. A Matlab script was applied to generate wavelet power spectra (Grinsted et al., 2004), and band-pass filtering was performed with AnalySeries (Paillard et al., 1996), centered at the dominant periodicities, with bandwidths at one fourth of the center frequency (details in the caption for Figure 3).

3. Results

3.1. Elemental Analyses

TOC contents at Site 364 vary significantly (Figure 1), from less than 1 wt % up to 40 wt %. Highest TOC contents occur in Unit 7b, which displays regularly paced variations between organic-lean carbonates with around 1 wt % TOC (typically ranging from 0.5% to 2 wt %) and sapropelic black shales with up to 40 wt % TOC (typically ranging from 10 to 25 wt %). Unit 7a is characterized by similar cyclic variations but with a lower maximum TOC content up to 11 wt %. Unit 6 consists predominately of carbonates with maximum TOC contents of 1–3 wt %. Elemental sulfur contents exhibit similar variations as TOC contents, with the maximum values of 11 wt % occurring in black shale horizons of Unit 7b and lower values in Units 7a and 6.

3.2. Time Series Analysis

The dominant periodicities in the depth domain over the whole Unit 7b TOC data set (Cores 42–45) are 46 and 73 cm (above the 99% confidence level; Figure 2, left panel). When analyzing only the upper part of the record from 1,024.62 to 1,037.92 m bsf (Cores 42 and 43), the dominant periodicity is again 46 cm (above the 99% confidence level; Figure 2, right panel), but a periodicity of 2.4 m can also be detected with more than 80% confidence. The differences between the power spectra of the entire record (revealing 46- and 73-cm periodicities) and that of only Cores 42 and 43 (46-cm and 2.4-m periodicity) are likely caused by

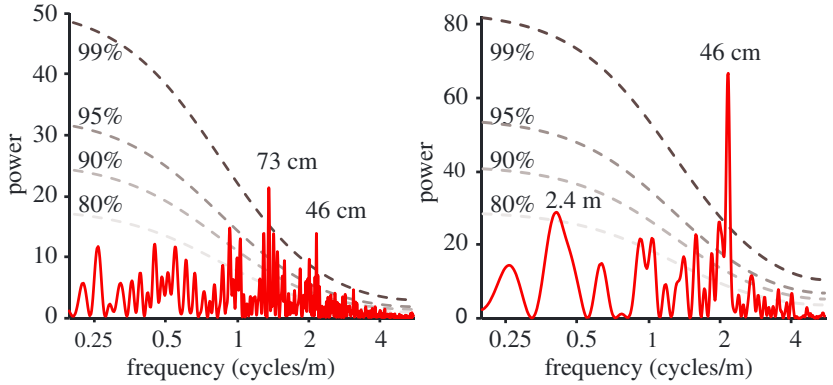

Figure 2. Redfit 3.8 power spectra of the total organic carbon record for the entirety of Unit 7b between 1,066 and 1,024 m below sea floor (left) and of the upper interval of Unit 7b only from 1,024 to 1,038 m below sea floor (right). Confidence levels are given in dashed lines, and dominant periodicities are labeled.

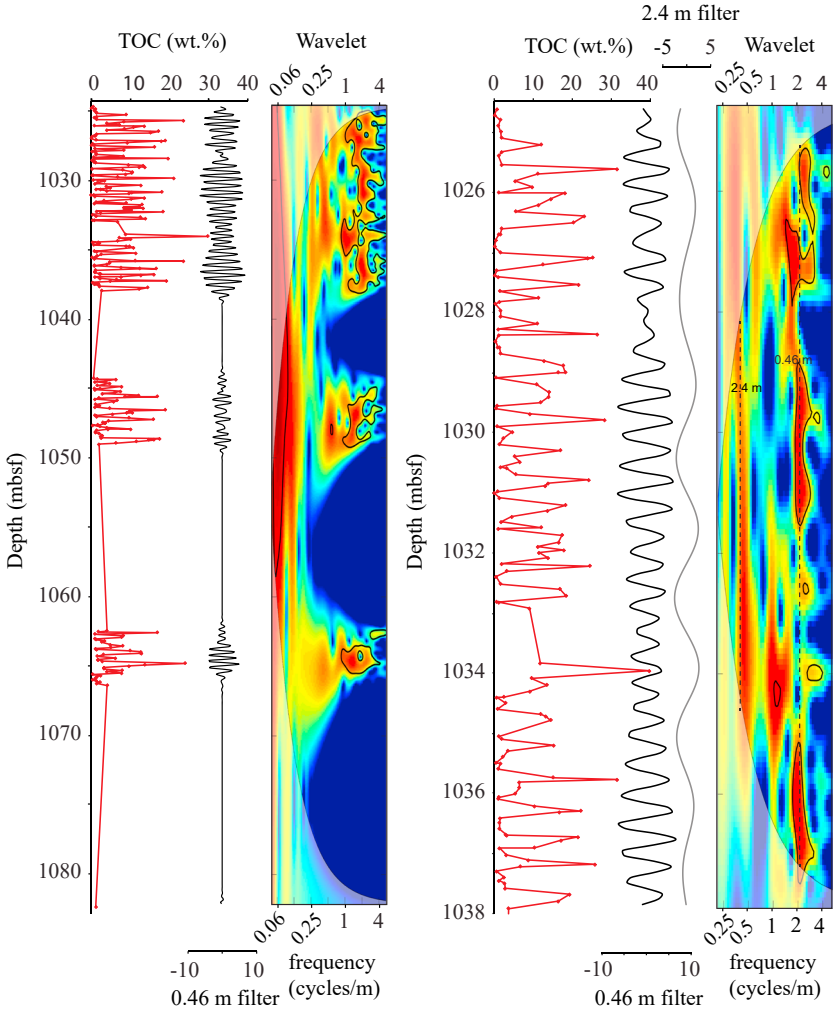

Figure 3. Total organic carbon (TOC) content and evolutionary spectra of the TOC record in the depth domain. The left figure shows the spectrum for the entirety of Unit 7b and depicts the band-pass filters centered at 0.46 m (bandwidth 0.37–0.60 m). The figure on the right spans only the upper part of Unit 7b and depicts the band-pass filters centered at 46 cm (bandwidth 0.37–0.61 m) and 2.4 m (bandwidth 1.9–3.2 m).

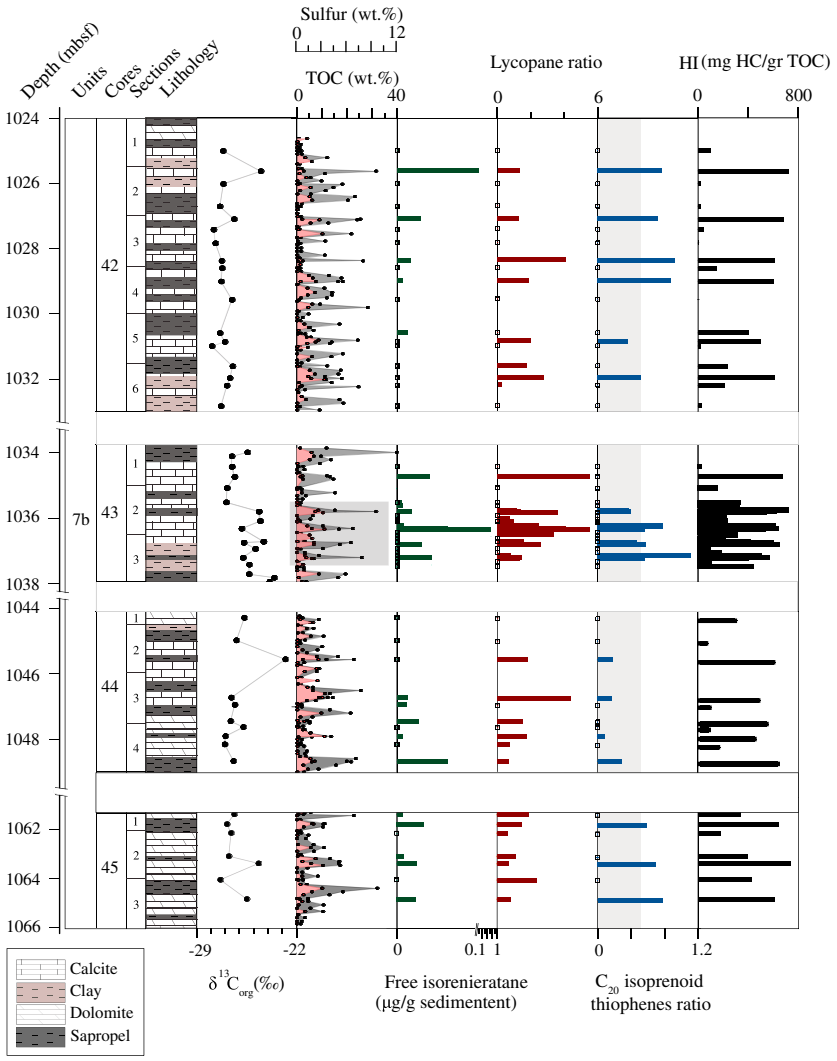

Figure 4. Lithology (Shipboard Scientific Party, 1984), bulk $\delta^{13}C_{org}$, total organic carbon (TOC) content (gray), sulfur content (red), free isorenieratane, lycopane ratio, C20 isoprenoid, and hydrogen index (HI) across Unit 7b (1,066–1,024 m below sea floor) for Deep Sea Drilling Project Site 364. High-amplitude-short term cyclic variations are present in both TOC and sulfur content. The mechanisms are studied with a higher resolution (10 cm^{-1}) in four representative cycles (1,037.5–1,035.5 m below sea floor) from Core 43, highlighted by a gray band.

the core gaps in the longer record. The wavelet spectrum of TOC (Figure 3) confirms these findings, revealing the presence of 46-cm and 2.4-m periodicities from 1,024.62 to 1,037.92 m bsf (Cores 42 and 43; Figure 3, right panel) and the persistent presence of the 46-cm periodicity through all of Unit 7b TOC data set (Cores 42–45), where data are available (Figure 3, left panel).

3.3. Rock-Eval

HIs for Unit 7b range from undetectable in some organic-lean carbonates to 740 mg HC/g TOC in black shales (Figure 4). In the organic-rich black shales, bulk OM is hydrogen-rich (HI on average ~ 440) type I/II kerogen, whereas in carbonates with low TOC, OM is dominated by oxygen-enriched but hydrogen-depleted (mean HI ~ 110) type III kerogen. T_{max} values range from 387 to 440 °C and are generally lower in black shales (mean ~ 395) than carbonates (mean ~ 420).

3.4. TOC Stable Carbon Isotopes ($\delta^{13}C_{org}$)

Bulk $\delta^{13}C_{org}$ values vary between −28 and −24‰ across Unit 7b (Cores 45–42; Figure 1). There is no variation with lithology, but the $\delta^{13}C_{org}$ record does exhibit a 2‰ positive excursion in Sections 2 and 3 of Core 43 at

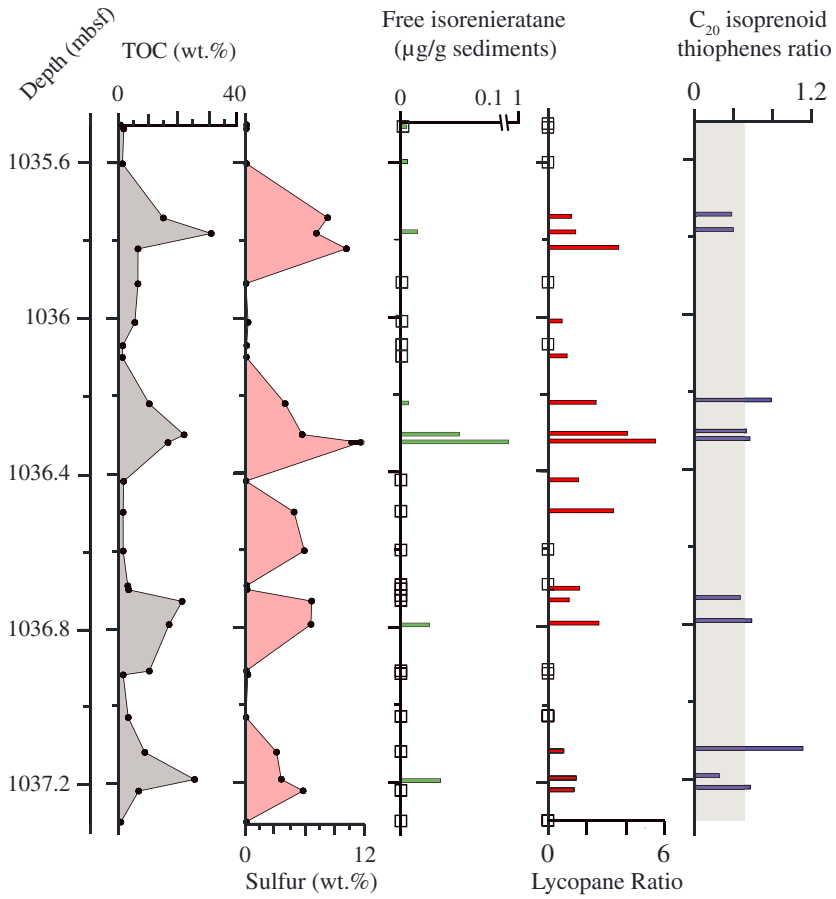

Figure 5. Total organic carbon (TOC) content (gray), sulfur content (red), free isorenieratane, lycopane ratio, and C_{20} isoprenoid for the four representative cycles of Unit 7b, with a high-resolution sampling (10 cm^{-1}). The peak in TOC cycles correspond to the maximum abundance of isorenieratane and lycopane (photic zone euxinia and water column anoxia) and the minimum of C_{20} isoprenoid thiophene ratio (hypersalinity).

around 1,035 m bsf (Figure 1). The $\delta^{13}C_{org}$ values in the upper parts of the section (Units 7a and 6) are again stable but lower than those of Unit 7b with values between −26 and −24‰.

3.5. Aliphatic Compounds

As shown previously (Hartwig et al., 2012; Naafs & Pancost, 2014; Simoneit, 1978), the aliphatic hydrocarbon fractions contain a mixture of *n*-alkanes, isoprenoids (pristane and phytane), steranes, and hopanes. The organic-rich black shale aliphatic fraction comprises mainly short-chain *n*-alkanes (C_{14}–C_{21}) with no obvious odd-over-even predominance, long-chain (C_{25}–C_{37}) *n*-alkanes with a slight odd-over-even carbon preference index (CPI ~ 1.6), C_{27}–C_{35} hopanes, C_{27}– C_{29} regular steranes, and acyclic isoprenoids such as pristane (Pr) and phytane (Ph). The organic-lean carbonates are also dominated by short-chain *n*-alkanes (C_{16}–C_{21}) with no obvious carbon number preference and pristane (Pr) and phytane (Ph); also present are long-chain *n*-alkanes (C_{25}–C_{29}), C_{27}–C_{31} hopanes, and C_{27}–C_{29} regular steranes. The ratio of the short- to long-chain *n*-alkanes [C_{17}/(C_{17} + C_{31})] in both organic-rich and organic-lean intervals is ~0.9. The ratio of steranes (only the regular steranes; see below) to hopanes, expressed here as $\frac{\sum \text{Steranes } (C_{27}-C_{29})}{\sum \text{hopanes } (C_{27}-C_{31})}$, is higher in black shales (0.86, with a typical range between 0.6 and 1.5) than carbonates (0.76, with a typical range between 0.4 and 1; Figure 6). The C_{31} hopane maturity index (C_{31} $\frac{\beta\beta}{\beta\beta+\beta\alpha+\alpha\beta}$) in both organic-rich and organic-lean intervals is approximately 0.15; expressing the alternation in the biological stereochemistry in a significant portion of the hopane stereoisomers, consistent with the thermal maturity of the host strata. The acyclic isoprenoid, 2,6,10,15,19-PMI, derived from both methanotrophic (e.g., Pancost et al., 2000) and methanogenic (Schouten et al., 1997)

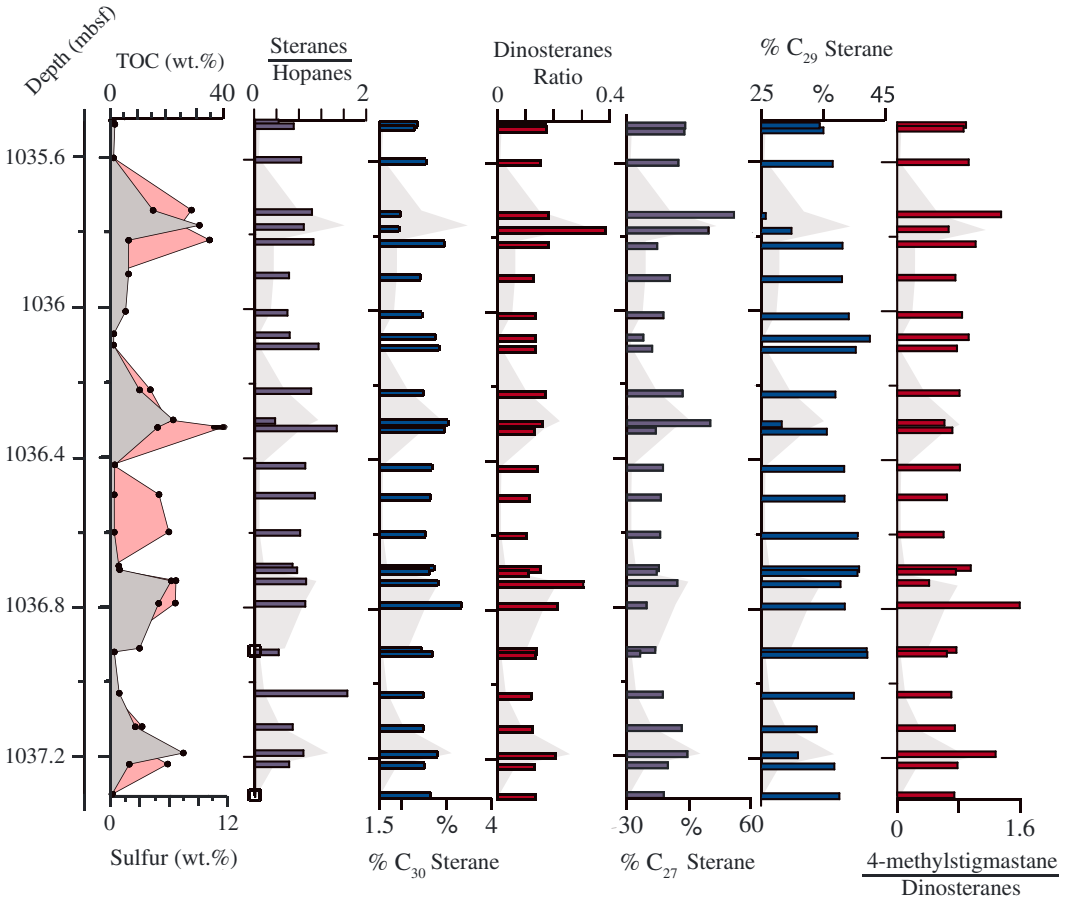

Figure 6. Total organic carbon (TOC) content (gray), sulfur content (red), C_{27}–C_{30} (24-*n*pc) steranes/C_{27} + C_{35} hopanes ratio, % C_{30} (24-*n*pc) sterane, dinoflagellate C_{30} methylsterane signal, % C_{27} and % C_{29} regular steranes, and 4-methylstigmastames/dinosteranes for the four representative cycles of Unit 7b, with a high-resolution sampling (10 cm^{-1}). Biomarkers distribution show that marine algal productivity was favored under photic zone euxinia condition, and stratification was established in the basin particularly when black shales were deposited.

Archaea, occurs in both lithologies. TOC-normalized concentrations of PMI in Cores 42–45 are higher in the carbonate intervals than the black shales (Figure 7). The $\delta^{13}C$ values of PMI in a black shale and carbonate samples from Unit 7b are −28‰ and −29‰, respectively. Lycopane is rarely present in carbonates and occasionally abundant in black shales of Unit 7b. The lycopane/C_{31} *n*-alkane ratio can be applied as a proxy for anoxic conditions in the water column (Sinninghe Damsté et al., 2003). Lycopane ratios are around 2 in black shales of Unit 7b but reach values as high as 5.5 in some horizons (Figures 4 and 5). Lycopane is largely absent in Units 7a and 6.

3.5.1. MRM (GC-MS-MS)

In addition to the aliphatic biomarkers, both organic-rich and organic-lean samples contain methylsteranes. However, due to low abundances and coelution, their identification required the use of MRM-GC-MS. As such, MRM-GC-MS was used to discriminate and confirm the presence of a full range of 4(α,β),23,24-trimethylcholestane isomers (dinosteranes, *m/z* 414 → 231 transition), 4(α,β)-methylstigmastanes (*m/z* 414 → 231 transition), and 24-*n*-propylcholestane (C_{30}, *m/z* 414 → 217 transition) and the commonly observed C_{27}–C_{29} regular steranes. Both regular and 4-methylsteranes occur in abundance in both organic-lean and organic-rich stratigraphic intervals and dominate 2-methylsterane and 3-methylsterane. However, the relative abundance of 24-*n*-propylcholestane (24-*n*pc) to C_{27}–C_{30} regular steranes varies between 2% and 3.5%, with the highest values in black shales (Figure 6). Similarly, the proportion of dinosteranes and 4-methylstigmastanes relative to total regular steranes and C_{30} 4-methylsteranes is generally higher in black shales (0.11–0.4) than in the carbonates (0.1–0.17, Figure 6). The proportion of

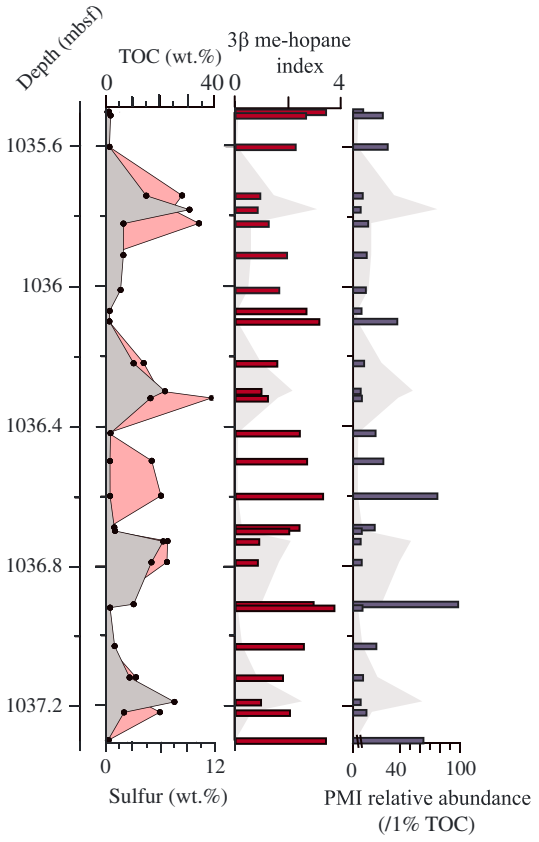

Figure 7. Total organic carbon (TOC) content (gray), sulfur content (red), 3β methylhopane index, and pentamethylicosane (PMI) relative abundance, for the four representative cycles of Unit 7b. The lower concentration of PMI in the aliphatic fractions of black shales than carbonates could be more attributed to the sulfur incorporation reactions rather than ecological changes.

4-methylstigmastanes relative to dinosteranes is higher in black shales (mean ~ 0.9) than in carbonates (mean ~ 0.7; Figure 6). MRM analysis also revealed trace abundances of 3β-methylhopanes (*m/z* 205) in both carbonates and black shales. The abundance of C_{31} 3β- methylhopane relative to C_{30} hopane and C_{31} 3β-methylhopane (3β-methylhopane index; $\left(\frac{C_{31}\ 3\beta-\text{methylhopanes}}{C_{31}\ 3\beta-\text{methylhopanes}+C_{30}\ \text{hopane}}\right)$) is generally higher in carbonates (2–4%) than black shales (<1–2%; Figure 7).

3.5.2. Thiophenes

The aliphatic hydrocarbon fractions also contain a series of *n*-alkyl and isoprenoidal thiophenes, organic sulfur compounds (Sinninghe Damsté & de Leeuw, 1990, and references therein). Both classes of thiophenes are largely absent in the organic-lean intervals. The C_{20} isoprenoid thiophene (*m/z* 308) is the most abundant isoprenoidal homolog. The C_{20} isoprenoid thiophene ratio ($\frac{\text{VII+VI}}{\text{I+II+III+IV+V}}$; for details see Figure 8) ranges between 0.2 and 1 (Figure 4).

3.6. Aromatic Compounds

The aromatic fraction from organic-rich intervals in Unit 7b comprises, among other compounds, isorenieratene, C_{35} hopane stereoisomers with thiophene rings, isoprenoid thiophenes, and isoprenoid thiolane. Of particular significance for this study is the presence of isorenieratane (*m/z* 546 and characteristic fragments of *m/z* 131 + 133), derived from isorenieratene, a carotenoid predominantly produced by phototrophic brown-pigmented green sulfur bacteria (*Chlorobiaceae*, Imhoff, 1995). Isorenieratane concentrations vary from 0 to 900 ng/g with highest values in organic-rich intervals (Figures 4 and 5). Although largely absent, isorenieratane also occurs in some of the organic-lean carbonates of Unit 7b (<6 ng/g; Figures 4 and 5). Isorenieratane was not detected in Units 7a and 6, including the black shales in those core sections.

3.7. Desulfurized Polar Compounds

Similar to the aliphatic fraction of organic-rich rocks, the apolar fraction of the desulfurized samples are dominated by short-chain *n*-alkanes (C_{16}–C_{21}) with no clear odd-over-even predominance, pristane (Pr) and phytane (Ph), PMI, lycopane (lycopane ratio ~ 1.4), and regular steranes (C_{27}–C_{29}, *S* and *R* isomers, base peak at *m/z* 217). Unlike the aliphatic fractions, long-chain (C_{25}–C_{40}) *n*-alkanes in desulfurized fractions do not exhibit any odd-over-even carbon preference index (CPI ~ 1). Moreover, the hopanes are dominated by the C_{35} homohopane, as is often the case for desulfurized polar fractions (e.g., de Leeuw & Sinninghe Damsté, 1990). Consistent with the composition of the aromatic fractions, the desulfurized polar fractions contain isorenieratane. Desulfurization also yielded chlorobactane (base peak at *m/z* 133, molecular ion *m/z* 554), a derivative of chlorobactene, derived from green-pigmented green sulfur bacteria, Chlorobiaceae (Imhoff, 1995).

4. Discussion

To explore the processes governing palaeoceanographic and carbon burial processes across multiple timescales, we first discuss the long-term decrease in TOC content from Unit 7b to Unit 6 (1,080–880 m bsf), considering it in the context of the opening phase of the South Atlantic Ocean (section 4.1). This is followed by a discussion that focuses on the short-term high-amplitude cyclic variations observed in the bulk records (TOC and S) and a high-resolution biomarker study of Unit 7b (1,080–1,025 m bsf), providing detailed insights in the depositional environment (section 4.2), the intensity of anoxia (section 4.3), and variations in the ecology (section 4.4) of the basin during the Aptian, methane cycling (section 4.5), and ultimately the processes behind these variations (section 4.6).

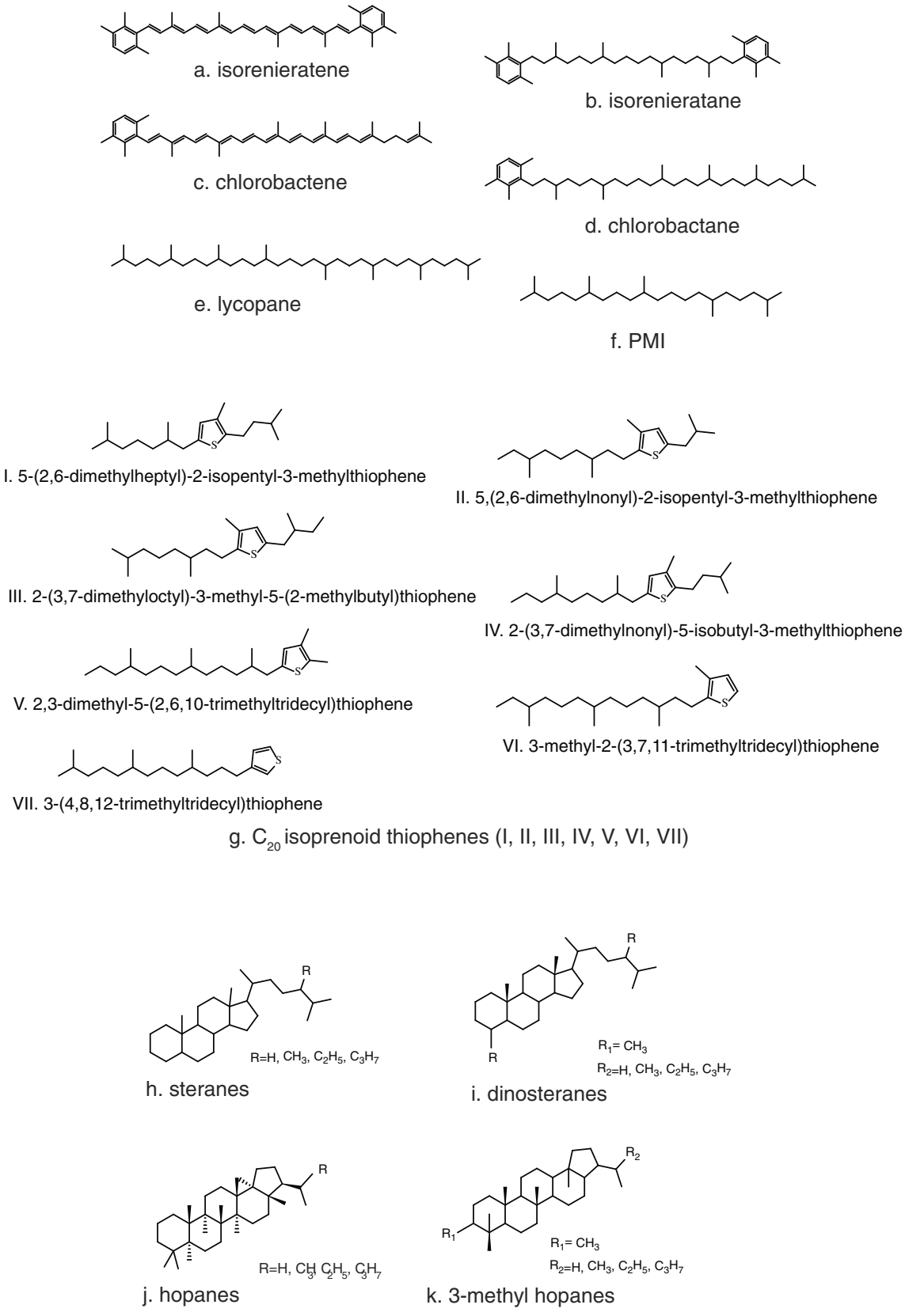

Figure 8. The schematic molecular structure of lipid biomarkers analyzed in this paper. (a) Isorenieratene, (b) isorenieratane, (c) chlorobactene, (d) chlorobactane, (e) lycopane, (f) pentamethylicosane (PMI), (g) C_{20} isoprenoid thiophenes, (h) steranes, (i) dinosteranes, (j) hopanes, and (k) 3-methyl hopanes.

4.1. Long-Term Redox Changes During the Opening of the South Atlantic

Unit 7b to Unit 6, spanning ~200 m of sediment of Aptian to late Aptian age, are characterized by relatively stable $\delta^{13}C_{org}$ values between −28‰ and −26‰ (Figure 1). However, sediments in Cores 44 and 43 (Unit 7b) demonstrate a ~2‰ shift to more positive values (Figures 1 and 4). This positive CIE could be interpreted as a reflection of enhanced carbon burial, and considering the age of these sediments (Aptian), it could potentially be attributed to the later stages of OAE 1a at around 120 Myr. OAE 1a is characterized by a brief negative and subsequent prolonged positive CIE (Menegatti et al., 1998) related to the input of isotopically light carbon into the ocean-atmospheric system and subsequent increased burial of ^{12}C-enriched OM. At Site 364 the positive CIE occurs directly above a ~13-m-long coring gap, which might explain the lack of a negative CIE that is characteristic for the onset of OAE 1a. As such, the sediments recovered in Cores 44 and 43 likely only represent the later stages of OAE 1a. Evidence of (the later part of) OAE 1a is also recorded in the evaporites of the Brazilian margin of the South Atlantic (Tedeschi et al., 2017).

The most significant characteristic of the Aptian–late Aptian sediments at Site 364 is the long-term decrease in (maximum) TOC content from Unit 7b (maximum 40 wt %) to Unit 7a (maximum 11 wt %) and Unit 6 (maximum 3 wt %). This change is accompanied by a parallel decrease in sulfur content (Figure 1). Although present in Unit 7b, the biomarker isorenieratane, indicative of photic zone euxinia (e.g., Koopmans et al., 1996), is absent in Units 7a and 6. The absence of lycopane, a biomarker predominantly produced in anoxic zones (Sinninghe Damsté et al., 2003, and references therein), in Unit 6 is also consistent with an overall decrease in the intensity of anoxia/euxinia in the basin throughout the Aptian.

Although the rifting process initiated in the Late Jurassic (e.g., Sibuet et al., 1984, and references therein), recent studies suggest that the northern South Atlantic basins remained isolated from significant oceanic water influx from the south until the Late Cretaceous (Pérez-Diaz & Eagles, 2014; Pérez-Díaz & Eagles, 2017). The South Atlantic basins also remained restricted to the north until sometime between the Aptian and Campanian stages, when a north-south Atlantic connection became established (Kochhann et al., 2013) and gradually intensified (Friedrich & Erbacher, 2006; Voigt et al., 2013). We therefore attribute the long-term decrease in TOC content, intensity of anoxia, and disappearance of photic zone euxinia to the gradual opening of the South Atlantic, deepening of the basin, and an associated decrease in basin restriction, which changed the sensitivity of the basin to climatic and depositional perturbations.

Although restricted, the basin was not uniformly anoxic/euxinic during the deposition of Unit 7b, as revealed by the cyclicity in TOC contents and the rhythmic occurrence of biomarker evidence of anoxia/euxinia (discussed below). Evidently, the basin geometry, with limited connectivity to the open ocean, preconditioned it for climatically induced changes in productivity and anoxia, similar to the Mediterranean during the Quaternary (Menzel et al., 2003; Meyers, 2006; Rohling, 1994) or as seen in the Deep Ivorian Basin to the north (ODP Site 959) during the Coniacian to Santonian (Beckmann et al., 2005; Hofmann et al., 2003; Wagner & Pletsch, 1999). This paleodepositional model is discussed further in section 4.2.

4.2. High-Amplitude, Short-Term Cyclic Variations in TOC Contents and Rock-Eval HIs

Superimposed on the long-term changes in TOC and sulfur content and shifts in biomarker distribution are high-amplitude, short-term cyclic variations that are especially pronounced in Unit 7b (Figure 4). These cycles are most prominent in the high-resolution TOC record but are also visible in biomarker records (Figures 5–7). The power spectrum of the high-resolution TOC record from Unit 7b highlights the strong periodicity of organic-rich black shales with a regular spacing of 46 cm (Figures 2 and 3). The difference between the power spectra of the entirety of Unit 7b (Cores 42–45) and only Cores 42 and 43 likely stems from the large coring gaps in Unit 7b. Nonetheless, both records highlight the dominance of a 46-cm periodicity. This observation suggests that rhythmically paced changes in the depositional environment occurred in the basin during the Early Cretaceous. This cyclicity bears a strong resemblance to the astronomically paced formation of organic-rich sapropels at Deep Ivorian Basin (ODP Site 959) during the Coniacian (Beckmann et al., 2005); at Demerara Rise (Leg 207) during the Cenomanian–Turonian (Flögel et al., 2008; Hofmann & Wagner, 2011; Meyers et al., 2006); at Site 530 during the Cenomanian–Turonian (Arthur et al., 1984; Deroo et al., 1984; A. Forster et al., 2008; Stow & Dean, 1984); and at Site 1138 during the Cenomanian–Turonian (Dickson et al., 2017).

To constrain these cycles to specific astronomical frequencies requires rigorous age constraints. Unfortunately, these are not available for Site 364 because Unit 7b does not have a precisely defined chronology and is characterized by coring gaps. However, the black shale layers appear to cluster in groups of five in the upper part of the section (Cores 42–45), bundled within the longer 2.4-m cycles (Figures 2 and 3). Based on this cycle hierarchy, and considering the subtropical location of Site 364 (~25°S), we suggest that changes in depositional environment are related to eccentricity-modulated precession, where the primary periodicity of 46 cm likely reflects the influence of precession (~21 kyr), and the 2.4-m periodicity may reflect the short eccentricity modulation of precession (~100 kyr). Below, we use detailed biomarker data to probe changes in the depositional environmental of the northern South Atlantic basin during the Aptian and across individual cycles.

4.3. Redox Changes Associated With Cyclicity in Unit 7b

Multiple lines of evidence indicate that significant redox changes accompany the black shale-carbonate cyclicity at Site 364; these include the laminations and high sulfur contents in the black shales (Figures 1 and 4) as well as observations that they are devoid of or contain poorly preserved benthic foraminifera specimens (Kochhann et al., 2014; Leg 40 Shipboard Scientific Party, 1978). In addition, the pattern of lower HI and higher T_{max} in the carbonates strongly suggests development of more oxic diagenetic conditions when organic-lean sediments were deposited (Landais et al., 1991; Stein, 1991). Here we explore evidence for the intensity of redox changes and their impact on OM character using biomarkers for sedimentary and water column redox conditions. These biomarkers provide evidence that low-oxygen or even euxinic conditions extended into the water column (and photic zone) during intervals of black shale deposition. First, lycopane mainly occurs in black shales, with particularly high lycopane ratios (up to 5.5) in some horizons indicating low-oxygen condition or anoxia in the water column (Sinninghe Damsté et al., 2003). Lycopane is not detected in most carbonate intervals, indicative of an oxygenated water column during periods of carbonate formation.

The interpretation of a lower water column oxygenation during black shale deposition is further supported by the presence of thiophene compounds such as C_{20} isoprenoid (midchain) thiophenes. Organic sulfur compounds are thought to be formed under euxinic conditions (Sinninghe Damsté et al., 1989). Their distribution ($(\frac{VII+VI}{I+II+III+IV+V})$; for details see Figure 8) has been proposed as an indicator of changes in salinity (Sinninghe Damsté et al., 1989; Sinninghe Damsté & de Leeuw, 1990). The C_{20} isoprenoid thiophenes ratio, although variable across the record, suggests episodes of hypersalinity and stratification in some, but not all, euxinic periods (Figures 4 and 5).

Euxinia likely extended into the photic zone, as indicated by the presence of isorenieratane, a derivative of carotenoids of green sulfur bacteria (Imhoff, 1995; Koopmans et al., 1996). Isorenieratene originates from brown strains of photosynthetic green sulfur bacteria (chlorobiacae; Imhoff, 1995, and references therein) that thrive near the chemocline at depths of up to 150 m, where the light levels are less than 1% of sea surface irradiance (Imhoff, 1995). In addition, the one desulfurized black shale sample contained chlorobactane. Chlorobactene is exclusively produced by the green strain of green sulfur bacteria (Imhoff, 1995, and references therein), which requires higher light intensity and thrives at shallower depths ($<$15 m; Imhoff, 1995, and references therein). Assuming a similar light dependence for these phototrophic sulfur bacteria during the Early Cretaceous, the presence of chlorobactane indicates that the chemocline occasionally extended to very shallow depths during black shale deposition, although the limited number of samples we desulfurized precludes us from concluding that these conditions occurred during the deposition of all black shales. Altogether, the biomarker assemblage provides compelling evidence that during deposition of Unit 7b, the northern South Atlantic water column periodically became profoundly depleted in oxygen, with anoxia and euxinia extending from the sediments to the (shallow) photic zone. Moreover, the basin was anoxic before, during, and after the potential OAE 1a positive CIE, resembling conditions that have been reported from other basins during the Cretaceous (e.g., Site 959; Beckmann et al., 2005; Hofmann et al., 2003; Wagner & Pletsch, 1999).

4.4. Biomarker Evidence of Cyclical Changes in Ecology

The high OM preservation and reducing conditions during the deposition of black shales could have resulted from increased marine productivity which would have dynamically maintained a redox-stratified water

column. This mechanism is consistent with the cyclic variations in the absence/presence and/or changes in the distribution of marine plankton community markers (Figure 6). For example, the abundance of (mainly) algal-derived steranes relative to bacterially derived hopanes, expressed as sterane/hopane ratio (Summons et al., 2006, and references therein), are slightly elevated in the black shales (mean ~ 0.86) compared to carbonates (mean ~ 0.76; Figure 6). Consistent with this ecological change is the higher concentration of C_{30} steranes (24-*n*pc) and particularly high (maximum ~ 0.4) dinoflagellate C_{30} methylsterane signal (dinosteranes and 4-methylstigmastanes) in the organic-rich black shales (Figure 6). The C_{30} regular sterane (24-npc) is a biomarker for predominantly marine pelaogophyte algae in Devonian and younger sedimentary rocks (e.g., Cao et al., 2009), whereas dinosteranes are mainly derived from marine dinoflagellates in Mesozoic and younger rocks and oils (e.g., Summons et al., 1992). Cyclic changes in water column ecology are also indicated by the predominance of C_{27} over all regular steranes (C_{27}–C_{30} (24-*n*pc)) in black shales, a distribution that changes to a predominance of C_{29} regular sterane in carbonates (Figure 6). Numerous studies of regular sterane (C_{27}–C_{29}) distributions and their specific precursors (W. Y. Huang & Meinschein, 1979; Kodner et al., 2008; Volkman et al., 1994) have led to various suggestions regarding their utility in inferring changes in OM source (although such approaches must be done cautiously, e.g., Kodner et al., 2008). For instance, the C_{27} and C_{29} sterols are preferentially synthesized by red algae and green algae, respectively (e.g., W. Y. Huang & Meinschein, 1979; Volkman et al., 1994; but see Kodner et al., 2008, for exceptions). Classically, higher relative abundances of C_{29} regular steranes have been interpreted as evidence of proportionally greater terrigenous inputs. Therefore, the observed variations in sterane distribution provide further evidence for ecological and/or OM source change, but the specific meaning of these changes is difficult to detangle. A shift to C_{27} sterane predominance is, however, consistent with a pulse of dinoflagellate activity during black shale deposition as dinoflagellates are from a derived red algal clade and C_{27} steranes are their major regular sterane marker (Volkman et al., 1994). The proportion of 4-methylstigmastane over dinosteranes as a signal of lacustrine fresh water (Goodwin et al., 1988; Hou et al., 2000; Summons et al., 1992, 1987) is higher in black shales (mean ~ 0.9) than carbonates (mean ~ 0.78; Figure 6). 4-Methylstigmastane and dinosteranes are indicators for marine (Goodwin et al., 1988; Moldowan et al., 1985; Summons et al., 1987) and nonmarine dinoflagellates (Jiamo et al., 1990). The dominance of 4-methylstigmastane over dinosteranes in our samples strongly suggests a lacustrine fresh water origin (Goodwin et al., 1988; Hou et al., 2000; Summons et al., 1992, 1987). 4-Methylstigmastanes are not selective biomarkers of dinoflagellates (Volkman et al., 1990); however, considering the higher proportion of C_{27} regular sterane in black shales, dinoflagellates are the likely source of 4-methylstigmastane (Fowler & McAlpine, 1995) in black shales. The dominance of 4-methylstigmastane in black shales (Figure 6) indicates the establishment of fresh (lower salinity) surface water layer and stratification in the basin particularly during the periods of enhanced terrestrial input and during the deposition of black shales, although the system remained marine (C_{30} regular steranes). Altogether, the biomarker evidence, alongside the high HIs in black shales, indicates that high marine algal productivity drove the water column anoxic/euxinic in a restricted basin, likely aided by elevated nutrient inputs and stratification.

4.5. Methane Cycling in Aptian South Atlantic

Other changes in basin ecology are documented by the abundances of microbial biomarkers, providing insights into the Aptian methane cycle in the northern South Atlantic. Compound-specific $\delta^{13}C$ of the archaeal lipid PMI ($\delta^{13}C_{PMI}$; see section 3.5) suggests a methanogenic rather than methanotrophic archaeal origin in this setting (e.g., Schouten et al., 1997). Concentrations of PMI are higher in the organic-lean carbonates than in the black shales (Figure 7). However, the desulfurized polar fraction of the black shale sample is also dominated by PMI, and the lower concentration of PMI in the aliphatic fraction of black shales is likely due to rapid sulfurization of PMI's highly unsaturated precursor during the early stages of diagenesis (sulfur incorporation reactions; Sinninghe Damsté & de Leeuw, 1990, and references therein), rather than ecological changes. Our data suggest that methanogenesis as the final step of OM biodegradation was occurring consistently in both carbonates and black shales.

Another aspect to consider is the concentration of 3β-methylhopanes in both carbonates and black shales (Figure 7). The most likely source of 3β-methylhopanes in marine environments is Type I methanotrophs (reviewed by Farrimond et al., 2004). This assumption can be supported by depleted carbon isotope compositions (Ruble et al., 1994), but that was not possible here due to overall low concentrations of this

biomarker. Methanotrophs are methane-oxidizing bacteria that tend to live under microaerophilic conditions, such as the chemocline in stratified environments (Hanson & Hanson, 1996). Because the 3β-methylhopane ratios are low (1%–4%) throughout the entire studied section and in the typical range for Phanerozoic sediments (1%–3%; Cao et al., 2009; i.e., there is no evidence for particularly enhanced abundances of aerobic methanotrophic bacteria), we suggest that the primary mode of methane oxidation was likely via anaerobic oxidation of methane (e.g., Orphan et al., 2002), similar to what has been previously reported for the Black Sea water column (Wakeham et al., 2003). However, the elevation of the 3β-methylhopanes ratio $\left(\frac{C_{31}\ 3\beta-\text{methylhopanes}}{C_{31}\ 3\beta-\text{methylhopanes}+C_{30}\ \text{hopane}}\right)$ by ~2% in carbonates, when the water column was more oxygenated, suggests that different bacterial communities (potentially type I methanotrophic bacteria; reviewed by Farrimond et al., 2004) prevailed during carbonate deposition. We suggest that aerobic methanotrophy dominated during these times, whereas anaerobic oxidation of methane was more important when the water column was largely anoxic.

4.6. Causes of Sedimentary Cycles

As discussed above, during the initial opening stages of the northern South Atlantic, sedimentary deposition was characterized by putatively cyclic burial of OM, reflecting a regular alternation between oxic and anoxic/euxinic conditions. Crucially, the cyclic changes in the concentrations of lycopane and isorenieratane confirm that these variations were not restricted to sediments or bottom waters but extended into the water column and even photic zone. We attribute these cyclical (precession-driven) changes primarily to increased stratification but also increased productivity during black shale deposition, the latter inferred from changes in algal biomarker assemblages that document ecological change. Enhanced productivity was likely driven by an increased input of biolimiting nutrients.

Wagner et al. (2013) presented a conceptual framework for the formation of proto Atlantic black shales in the (sub)tropics during the Cretaceous (Albian, Cenomanian–Turonian), linking the richness and quality of OM to changes in upwelling in the proto-Atlantic and continental runoff into the basin. However, in modern upwelling regions such as off the coast of Peru (Dugdale et al., 1977) and those in the Indian Ocean (Ivanenkov & Rozanov, 1961) photic zone euxinia does not occur; furthermore, isoreniaretane (or its biological precursor isoreniaratene) is only found in the sediments and water column of stratified basins such as the Black Sea (Repeta et al., 1989). We therefore argue that the occurrence of anoxic/euxinic conditions during deposition of the Aptian black shale horizons at Site 364 was probably related to water column stratification combined with enhanced primary productivity driven by terrestrial nutrient delivery. This situation is similar to what has been invoked for the formation of Coniacian-Santonian black shales (ODP Site 959) in the tropics (Beckmann et al., 2005; Flögel & Wagner, 2006; Wagner et al., 2013) and Albian black shale deposits of DSDP Site 367 in the eastern North Atlantic (Hofmann et al., 1999; Wagner et al., 2013). This hypothesis is further supported by the dominance of 4-methylsteranes in C_{30} methylsteranes as an evidence for salinity stratification (Goodwin et al., 1988) in both carbonates and black shales. Additionally, the proportion of 4-methylstigmastane over dinosteranes in black shales (Figure 6) as a signal of lacustrine fresh water layer (Goodwin et al., 1988; Hou et al., 2000; Summons et al., 1987, 1992) and establishment of stratification in the basin, is particularly higher during the periods black shale deposited. In addition, overall low ($<$0.5) C_{20} isoprenoid thiophene ratio in black shale horizons at Site 364 suggests episodes of hypersalinity and stratification during (some of) the euxinic periods (Figures 4 and 5). Moreover, the pattern of HI and T_{max} values in carbonates and black shales proposes a significant background composition of transported terrestrial OM (kerogen type III) in the organic-lean carbonates. This is consistent with the pulses of high marine productivity dynamically maintaining reducing conditions within the water column during the deposition of black shales (kerogen type II).

We argue that Aptian organic-rich black shales (with high HI values) in Site 364 represent the strong influence of continental runoff from tropical South Africa, whereas carbonate horizons with low organic content (and low HI values) formed when the basin was influenced from the SW trade winds and more oxic conditions developed (when the Intertropical Convergence Zone was located in a relatively northern position). Climate model simulations support our hypothesis, demonstrating that the appearance of the Atlantic Ocean led to significant changes in the hydrological cycle and modulated the monsoonal-influenced regions (Ohba & Ueda, 2010).

Crucially, the impact of these climatic factors was modulated by the evolution of the South Atlantic, which resulted in the formation of series of rift basins in the (sub)tropics which gradually became connected to the open ocean through the (Early) Cretaceous (e.g., Friedrich & Erbacher, 2006; Pérez-Diaz & Eagles, 2014). These rift basins and the early restricted South Atlantic were particularly sensitive to orbitally controlled changes in monsoonal runoff and episodic formation of organic-rich black shales. To the best of our knowledge, there is no other Aptian-age black shale or modeling study in the South Atlantic to help us build a wider concept regarding the formation of black shales in the region. However, our findings shed some light on the sedimentary pattern of Aptian black shales deposition, and in particular, they support the hypothesis that changes in organic carbon richness is controlled by orbitally paced variations in the hydrological cycle, as has been inferred for the Cretaceous (Hofmann & Wagner, 2011; Wagner et al., 2013) and Jurassic (Armstrong et al., 2016). Based on our results from Site 364 we argue that the southward development of the Intertropical Convergence Zone (~25°S) during the Aptian alongside with the paleogeography of the region made the South Atlantic sensitive to the orbitally forced variations in hydrology and likely led to a widespread occurrence of Aptian black shales in the South Atlantic. A strength of the hydrologically modulated mechanism is that it would have not only enhanced nutrient inputs but could have contributed to density-driven water column stratification. This combination of enhanced productivity and stratification-limited oxygenation of deep waters could have combined to generate the particularly dramatic changes in TOC content and character, as has been invoked for Site 959 (ODP Leg 159; the deep Ivorian Basin; e.g., Wagner & Pletsch, 1999). Previous work (Słowakiewicz et al., 2015) has cautioned against interpreting basin-scale stratification on the basis of a single site, but the particularly high TOC contents observed here do suggest changes in productivity and ocean circulation. Crucially, the cyclic burial of such organic-rich sediments appears to have stimulated a particularly strong methane cycle. The very high concentration of PMI in desulfurized black shale extracts suggests intense methanogenesis in those horizons, whereas the 3β-methylhopanes provide evidence for aerobic methanotrophy, perhaps in the water column. Altogether, the carbon cycle in the northern South Atlantic during the Aptian seems to have been controlled by astronomical forcing (precession), driving changes in the hydrological cycle that subsequently regulated the methane cycle via biodegradation of OM.

Although our results are specific to Site 364 and the margins of northern South Atlantic, periodic black shales of similar age (Early Cretaceous) have been reported elsewhere in the proto-Atlantic, for example, at Site 530 in the Angola basin (e.g., Deroo et al., 1984; Katz, 1984; Meyers et al., 1984; Rullkötter et al., 1984; Stow & Dean, 1984); Site 511 in the Falkland Plateau (e.g., Deroo et al., 1983), and Site 367 in Gambia Abyssal Plain (e.g., Hofmann et al., 1999; Wagner et al., 2013). There are also numerous publications on the astronomically controlled formation of black shales in the Late Cretaceous, for example, from Site 959 in the Ivorian Basin (Beckmann et al., 2005; Holbourn et al., 1999), Leg 207 (Sites 1257–1261) at Demerara Rise (Hofmann & Wagner, 2011; Meyers et al., 2006), Site 530 in the Angola basin (e.g., Arthur et al., 1984; Deroo et al., 1984; A. Forster et al., 2008; Stow & Dean, 1984), the Western Interior Seaway (Eldrett et al., 2015), and ODP Site 1138 in the Indian Ocean (Dickson et al., 2017). These results suggest that the proposed depositional mechanism for Site 364 of a hydrographically restricted basin that was preconditioned to astronomically controlled variations in terrestrial runoff was probably a common feature of the proto-Atlantic region during the Cretaceous. These observations highlight the strong links between climate, the hydrological cycle, terrestrial weathering, nutrient availability, primary production, and deoxygenation in the marine system.

5. Conclusions

High-resolution geochemical data from DSDP Site 364 (Units 7b to 6) allow reconstruction of the intensity and persistence of redox conditions in the northern South Atlantic Ocean during its early opening phase in the Aptian. The opening history of the northern South Atlantic is documented by the accumulation of organic carbon, with the relatively high preservation of OM in the restricted basin (Unit 7b and to a less extent in unit 7a), terminated by continued rifting, basin deepening, and increased connectivity with the open ocean by the late Aptian (Unit 6). High-amplitude fluctuations in TOC and total sulfur contents and HIs indicate that basin restriction alone did not cause anoxic conditions to develop but instead preconditioned the basin for oxygen depletion during episodes of enhanced OM production and export. Productivity fluctuations most likely resulted from eccentricity-modulated precession changes in the delivery of biolimiting

nutrients from weathering and terrestrial runoff. Enhanced terrestrial runoff, perhaps associated with a strengthened hydrological cycle, might also have caused salinity stratification in the upper ocean, as evidenced by elevated proportion of 4(αβ)-methylstigmastane over dinosteranes during the periods of increased terrestrial input and also cyclic variations in C_{20} isoprenoid thiophene abundances. Regardless of the forcing mechanism(s), the impact of cyclical changes in climate on the South Atlantic was pronounced, evidenced by increased primary production and changes in algal assemblages; anoxic conditions in the water column, including photic zone euxinia and sometimes extending to very shallow water depths (<15 m); and a pronounced methane cycle.

Acknowledgments
This research was funded through the advanced ERC grant *The GReenhouse Earth System* (T-GRES, project reference 340923), awarded to R. D. P. We would like to thank G. N. Inglis and S. K. Lengger for help with desulfurization of polar fraction and M. Rohrssen for helpful discussions. Philip A. Meyers and an anonymous reviewer are acknowledged for their constructive suggestions and valuable feedback. The authors wish to thank NERC for partial funding of the mass spectrometry facilities at Bristol (contract R8/H10/63; www.lsmsf.co.uk). D. Davis and S. Nicoara are acknowledged for elemental and bulk $\delta^{13}C_{org}$ analyses. The International Ocean Discovery Program (IODP) provided sample material. Data from this study can be found in the supporting information (Table S1).

References

Armstrong, H. A., Wagner, T., Herringshaw, L. G., Farnsworth, A. J., Lunt, D. J., Harland, M., et al. (2016). Hadley circulation and precipitation changes controlling black shale deposition in the Late Jurassic boreal seaway. *Paleoceanography*, *31*, 1041–1053. https://doi.org/10.1002/2015PA002911

Arthur, M. A., Dean, W. E., & Stow, D. A. V. (1984). Models for the deposition of Mesozoic-Cenozoic fine-grained organic-carbon-rich sediment in the deep sea. *Geological Society, London, Special Publications*, *15*(1), 527–560. https://doi.org/10.1144/GSL.SP.1984.015.01.34

Beckmann, B., Flogel, S., Hofmann, P., Schulz, M., & Wagner, T. (2005). Orbital forcing of Cretaceous river discharge in tropical Africa and ocean response. *Nature*, *437*(7056), 241–244. https://doi.org/10.1038/nature03976

Bice, K. L., Birgel, D., Meyers, P. A., Dahl, K. A., Hinrichs, K. U., & Norris, R. D. (2006). A multiple proxy and model study of Cretaceous upper ocean temperatures and atmospheric CO_2 concentrations. *Paleoceanography*, *21*, PA2002. https://doi.org/10.1029/2005PA001203

Bralower, T. J., Arthur, M. A., Leckie, R. M., Sliter, W. V., Allard, D. J., & Schlanger, S. O. (1994). Timing and paleoceanography of oceanic dysoxia/anoxia in the late Barremian to early Aptian (Early Cretaceous). *PALAIOS*, *9*(4), 335–369. https://doi.org/10.2307/3515055

Cao, C., Love, G. D., Hays, L. E., Wang, W., Shen, S., & Summons, R. E. (2009). Biogeochemical evidence for euxinic oceans and ecological disturbance presaging the end-Permian mass extinction event. *Earth and Planetary Science Letters*, *281*(3-4), 188–201. https://doi.org/10.1016/j.epsl.2009.02.012

de Leeuw, J. W., & Sinninghe Damsté, J. S. (1990). Organic sulfur compounds and other biomarkers as indicators of palaeosalinity. In W. L. Orr & C. M. White (Eds.), *Geochemistry of sulfur in fossil fuels* (pp. 417–443). Washington, DC: American Chemical Society. https://doi.org/10.1021/bk-1990-0429.ch024

Deroo, G., Herbin, J. P., & Huc, A. Y. (1984). Organic geochemistry of Cretaceous black shales from Deep Sea Drilling Project Site 530, Leg 75, Eastern South Atlantic. In W. W. Hay, et al. (Eds.), *Initial reports of the Deep Sea Drilling Project; part V: Organic geochemistry* (pp. 983–999). Washington, DC: U.S. Government Printing Office. https://doi.org/10.2973/dsdp.proc.75.130.1984

Deroo, G., Herbin, J. P., & Roucaché, J. (1983). 37. Organic geochemistry of Upper Jurassic-Cretaceous sediments from Site 511, Leg 71, western South Atlantic. In W. J. Ludwig, V. A. Krasheninnikov, & E. Al (Eds.), *Initial reports of the Deep Sea Drilling Project 41. U.S. government printing office* (pp. 1001–1013). Paris, France: Institut Français du Pétrole. https://doi.org/10.1594/PANGAEA.815172

Dickson, A. J., Saker-clark, M., Jenkyns, H. C., Bottini, C., Erba, E., Russo, F., et al. (2017). A Southern Hemisphere record of global trace-metal drawdown and orbital modulation of organic-matter burial across the Cenomanian – Turonian boundary (ocean drilling program Site 1138, Kerguelen Plateau). *Sedimentology*, *64*, 186–203. https://doi.org/10.1111/sed.12303

Dugdale, R. C., Goering, J. J., Barber, R. T., Smith, R. L., & Packard, T. T. (1977). Denitrification and hydrogen sulfide in the Peru upwelling region during 1976. *Deep Sea Research*, *24*(6), 601–608. https://doi.org/10.1016/0146-6291(77)90530-6

Eldrett, J. S., Ma, C., Bergman, S. C., Ozkan, A., Minisini, D., Lutz, B., et al. (2015). Origin of limestone-marlstone cycles: Astronomic forcing of organic-rich sedimentary rocks from the Cenomanian to early Coniacian of the Cretaceous Western Interior Seaway, USA. *Earth and Planetary Science Letters*, *423*, 98–113. https://doi.org/10.1016/j.epsl.2015.04.026

Farrimond, P., Talbot, H. M., Watson, D. F., Schulz, L. K., & Wilhelms, A. (2004). Methylhopanoids: Molecular indicators of ancient bacteria and a petroleum correlation tool. *Geochimica et Cosmochimica Acta*, *68*(19), 3873–3882. https://doi.org/10.1016/j.gca.2004.04.011

Flögel, S., Beckmann, B., Hofmann, P., Bornemann, A., Westerhold, T., Norris, R. D. D., et al. (2008). Evolution of tropical watersheds and continental hydrology during the Late Cretaceous greenhouse; impact on marine carbon burial and possible implications for the future. *Earth and Planetary Science Letters*, *274*(1-2), 1–13. https://doi.org/10.1016/j.epsl.2008.06.011

Flögel, S., & Wagner, T. (2006). Insolation-control on the Late Cretaceous hydrological cycle and tropical African climate-global climate modelling linked to marine climate records. *Palaeogeography, Palaeoclimatolology, Palaeoecology*, *235*(1-3), 288–304. https://doi.org/10.1016/j.palaeo.2005.09.034

Foresman, J. B. (1984). Organic geochemistry DSDP Leg 40, continental rise of southwest Africa. In *Deep Sea Drilling Projects and publications; part III: Organic geochemistry* (pp. 557–567). Washington, DC: US Government Printing Office. https://doi.org/10.2973/dsdp.proc.40.111.1978

Forster, A., Kuypers, M. M. M., Turgeon, S. C., Brumsack, H.-J., Petrizzo, M. R., & Sinninghe Damsté, J. S. (2008). The Cenomanian/Turonian oceanic anoxic event in the South Atlantic: New insights from a geochemical study of DSDP Site 530A. *Palaeogeography Palaeoclimatolology Palaeoecology*, *267*(3-4), 256–283. https://doi.org/10.1016/j.palaeo.2008.07.006

Foster, G. L., Royer, D. L., & Lunt, D. J. (2017). Future climate forcing potentially without precedent in the last 420 million years. *Nature Communications*, *8*. https://doi.org/10.1038/ncomms14845

Fowler, M. G., & McAlpine, K. D. (1995). The egret member, a prolific Kimmeridgian source rock from offshore eastern Canada. In B. J. Katz (Ed.), *Petroleum source rocks. casebooks in Earth sciences* (pp. 111–130). Berlin: Springer. https://doi.org/10.1007/978-3-642-78911-3_7

Friedrich, O., & Erbacher, J. (2006). Benthic foraminiferal assemblages from Demerara Rise (ODP Leg 207, western tropical Atlantic): Possible evidence for a progressive opening of the equatorial Atlantic gateway. *Cretaceous Research*, *27*(3), 377–397. https://doi.org/10.1016/j.cretres.2005.07.006

Goodwin, N. S., Mann, A. L., & Patience, R. L. (1988). Structure and significance of C_{30} 4-methyl steranes in lacustrine shales and oils. *Organic Geochemistry*, *12*(5), 495–506. https://doi.org/10.1016/0146-6380(88)90159-3

Grinsted, A., Moore, J. C., & Jevrejeva, S. (2004). Application of the cross wavelet transform and wavelet coherence to geophysical time series. *Nonlinear Processes in Geophysics*, *11*(5/6), 561–566. https://doi.org/10.5194/npg-11-561-2004

Hanson, R. S., & Hanson, T. E. (1996). Methanotrophic bacteria. *Microbiological Reviews*, *60*(2), 439–471.

Hartwig, A., di Primio, R., Anka, Z., & Horsfield, B. (2012). Source rock characteristics and compositional kinetic models of Cretaceous organic rich black shales offshore southwestern Africa. *Organic Geochemistry*, *51*, 17–34. https://doi.org/10.1016/j.OrganicGeochemistry.2012.07.008

Hay, W. W. (2008). Evolving ideas about the Cretaceous climate and ocean circulation. *Cretaceous Research*, *29*(5-6), 725–753. https://doi.org/10.1016/j.cretres.2008.05.025

Hofmann, P., Ricken, W., Schwark, L., & Leythaeuser, D. (1999). Coupled oceanic effects of climatic cycles from late Albian deep-sea sections of the North Atlantic. In E. Barrera & C. Johnson (Eds.), *The evolution of Cretaceous ocean/climate systems* (pp. 143–159). Colorado: Geological Society of America Special Publication. https://doi.org/10.1130/0-8137-2332-9.143

Hofmann, P., & Wagner, T. (2011). ITCZ controls on Late Cretaceous black shale sedimentation in the tropical Atlantic Ocean. *Paleoceanography*, *26*, PA002154. https://doi.org/10.1029/2011PA002154

Hofmann, P., Wagner, T., & Beckmann, B. (2003). Millennial- to centennial-scale record of African climate variability and organic carbon accumulation in the Coniacian–Santonian eastern tropical Atlantic (Ocean Drilling Program Site 959, off Ivory Coast and Ghana). *Geology*, *31*(2), 135–138. https://doi.org/10.1130/0091-7613(2003)031<0135:MTCSRO>2.0.CO;2

Holbourn, A., Kuhnt, W., El Albani, A., Pletsch, T., Luderer, F., & Wagner, T. (1999). Upper Cretaceous palaeoenvironments and benthonic foraminiferal assemblages of potential source rocks from the western African margin, Central Atlantic. *Geological Society London, Specific Publications*, *153*(1), 195–222. https://doi.org/10.1144/GSL.SP.1999.153.01.13

Hou, D., Li, M., & Huang, Q. (2000). Marine transgressional events in the gigantic freshwater lake Songliao: Paleontological and geochemical evidence. *Organic Geochemistry*, *31*(7-8), 763–768. https://doi.org/10.1016/S0146-6380(00)00065-6

Huang, C., Hinnov, L., Fischer, A. G., Grippo, A., & Herbert, T. (2010). Astronomical tuning of the Aptian stage from Italian reference sections. *Geology*, *38*(10), 899–902. https://doi.org/10.1130/G31177.1

Huang, W. Y., & Meinschein, W. G. (1979). Sterols as ecological indicators. *Geochimica et Cosmochica Acta*, *43*(5), 739–745. https://doi.org/10.1016/0016-7037(79)90257-6

Huber, B. T., Norris, R. D., & MacLeod, K. G. (2002). Deep-sea paleotemperature record of extreme warmth during the Cretaceous. *Geology*, *30*(2), 123–126. https://doi.org/10.1130/0091-7613(2002)030<0123:DSPROE>2.0.CO;2

Imhoff, J. (1995). Taxonomy and physiology of phototrophic purple bacteria and green sulfur bacteria. In R. E. Blankenship, C. E. Madigan, & M. T. Bauer (Eds.), *Anoxygenic photosynthetic bacteria* (pp. 1–15). Printed in The Netherlands: Kluwer Academic Publishers. https://doi.org/10.1007/0-306-47954-0_1

Ivanenkov, B. H., & Rozanov, A. (1961). Hydrogen sulphide contamination of the intermediate water layers of the Arabian Sea and the Bay of Bengal. *Okeanologica Acta*, *1*(3), 443–449.

Jenkyns, H. C. (2010). Geochemistry of oceanic anoxic events. *Geochemistry, Geophysics, Geosystems*, *11*, Q03004. https://doi.org/10.1029/2009GC002788

Jenkyns, H. C., Schouten-Huibers, L., Schouten, S., & Sinninghe Damsté, J. S. (2012). Warm Middle Jurassic-Early Cretaceous high-latitude sea-surface temperatures from the Southern Ocean. *Climate of the Past*, *8*(1), 215–226. https://doi.org/10.5194/cp-8-215-2012

Jiamo, F., Guoying, S., Jiayou, X., Eglinton, G., Gowar, A. P., Rongfen, J., et al. (1990). Application of biological markers in the assessment of paleoenvironments of Chinese non-marine sediments. *Organic Geochemistry*, *16*(4-6), 769–779. https://doi.org/10.1016/0146-6380(90)90116-H

Katz, B. J. (1984). Organic geochemical character of selected cores, Deep Sea Drilling Project Hole 530A. In *Deep Sea Drilling Projects and publications; part V: Organic geochemistry* (pp. 1031–1034). Washington, DC: US Government Printing Office. https://doi.org/10.2973/dsdp.proc.75.134.1984

Kochhann, K. G., Koutsoukos, E. A. M., Fauth, G., & Sial, A. N. (2013). Aptian-Albian planktic foraminifera from DSDP Site 364 (offshore Angola): Biostratigraphy, paleoecology, and paleoceanographic significance. *The Journal of Foraminifera Research*, *43*(4), 443–463. https://doi.org/10.2113/gsjfr.43.4.443

Kochhann, K. G. D., Koutsoukos, E. A. M., & Fauth, G. (2014). Aptian-Albian benthic foraminifera from DSDP Site 364 (offshore Angola): A paleoenvironmental and paleobiogeographic appraisal. *Cretaceous Research*, *48*, 1–11. https://doi.org/10.1016/j.cretres.2013.11.009

Kodner, R. B., Pearson, A., Summons, R. E., & Knoll, A. H. (2008). Sterols in red and green algae: Quantification, phylogeny, and relevance for the interpretation of geologic steranes. *Geobiology*, *6*(4), 411–420. https://doi.org/10.1111/j.1472-4669.2008.00167.x

Koopmans, M. P., Köster, J., Van Kaam-Peters, H. M. E. E., Kenig, F., Schouten, S., Hartgers, W. A., et al. (1996). Diagenetic and catagenetic products of isorenieratene: Molecular indicators for photic zone anoxia. *Geochimica et Cosmochimica Acta*, *60*(22), 4467–4496. https://doi.org/10.1016/S0016-7037(96)00238-4

Kuypers, M. M. M., Lourens, L. J., Rijpstra, W. I. C., Pancost, R. D., Nijenhuis, I. A., & Sinninghe Damsté, J. S. (2004). Orbital forcing of organic carbon burial in the proto-North Atlantic during oceanic anoxic event 2. *Earth and Planetary Science Letters*, *228*(3-4), 465–482. https://doi.org/10.1016/j.epsl.2004.09.037

Landais, P., Michels, R., Kister, J., Derepge, J.-M., & Benkheddat, Z. (1991). Behavior of oxidized type II kerogen during artificial maturation. *Energy & Fuels*, *5*(6), 860–866. https://doi.org/10.1021/ef00030a014

Leg 40 Shipboard Scientific Party (1978). Angola continental margin_Sites 364 and 365. In H. M. Bolli, et al. (Eds.), *Initial reports of the Deep Sea Drilling Project* (pp. 357–455). Washington, DC: US Government Printing Office. https://doi.org/10.2973/dsdp.proc.40.104.1978

MacLeod, K. G., Huber, B. T., Berrocoso, Á. J., & Wendler, I. (2013). A stable and hot Turonian without glacial $\delta^{18}O$ excursions is indicated by exquisitely preserved Tanzanian foraminifera. *Geology*, *41*. https://doi.org/10.1130/G34510.1

Malinverno, A., Erba, E., & Herbert, T. D. (2010). Orbital tuning as an inverse problem: Chronology of the early Aptian oceanic anoxic event 1a (Selli level) in the Cismon APTICORE. *Paleoceanography*, *25*, PA2203. https://doi.org/10.1029/2009PA001769

Matsumoto, R., Utada, M., & Kagami, H. (1978). Sedimentary petrology of DSDP cores from Sites 362 and 353, the Walvis Ridge, and Site 364, the Angola Basin, drilled on Leg 40. In *Deep Sea Drilling Projects and publications; part II: Studies in sedimentology* (pp. 469–483). Washington, DC: US Government Printing Office. https://doi.org/10.2973/dsdp.proc.40.106.1978

Matsumoto, T., 1978. Notes on Inoceramus, Mesozoic bivalves from the southeastern Atlantic, DSDP Sites 361 and 364, Leg 40, in: Deep Sea Drilling Projects and publications; to volumes XXXVIII, XXXIX, XL, and XLI. Pp. 703–707. https://doi.org/10.2973/dsdp.proc.38394041s.311.1978

Menegatti, A. P., Weissert, H., Brown, R. S., Tyson, R. V., Farrimond, P., Strasser, A., & Caron, M. (1998). High-resolution ^{13}C stratigraphy through the early Aptian "Livello Selli" of the Alpine Tethys Alessio. *Paleoceanography*, *13*, 530–545. https://doi.org/10.1029/98PA01793

Menzel, D., Van Bergen, P. F., Schouten, S., & Sinninghe Damsté, J. S. (2003). Reconstruction of changes in export productivity during Pliocene sapropel deposition: A biomarker approach. *Palaeogeography Palaeoclimatology Palaeoecology*, *190*, 273–287. https://doi.org/10.1016/S0031-0182(02)00610-7

Meyers, P. A. (2006). Paleoceanographic and paleoclimatic similarities between Mediterranean sapropels and Cretaceous black shales. *Palaeogeography Palaeoclimatology Palaeoecology*, *235*(1-3), 305–320. https://doi.org/10.1016/j.palaeo.2005.10.025

Meyers, P. A., Bernasconi, S. M., & Forster, A. (2006). Origins and accumulation of organic matter in expanded Albian to Santonian black shale sequences on the Demerara Rise, South American margin. *Organic Geochemistry*, *37*(12), 1816–1830. https://doi.org/10.1016/j.orggeochem.2006.08.009

Meyers, P.A., Trull, T.W., Kawka, O.E., 1984. Organic Geochemical Comparison of Cretaceous Green and Black Claystones from Hole 530A in the Angola Basin, in: Deep Sea Drilling Projects and Publications; part V: Organic Geochemistry (pp. 1009–1018).

Moldowan, J., Seifert, W. K., & Gallegos, E. J. (1985). Relationship between petroleum composition and depositional environment of petroleum source rocks. *The American Association of Petroleum Geologists Bulletin*, *69*, 1255–1268.

Naafs, B. D. A., Castro, J. M., De Gea, G. A., Quijano, M. L., Schmidt, D. N., & Pancost, R. D. (2016). Gradual and sustained carbon dioxide release during Aptian oceanic anoxic event 1a. *Nature Geoscience*, *9*(2), 135–139. https://doi.org/10.1038/ngeo2627

Naafs, B. D. A., & Pancost, R. D. (2014). Environmental conditions in the South Atlantic (Angola Basin) during the Early Cretaceous. *Organic Geochemistry*, *76*, 184–193. https://doi.org/10.1016/j.orggeochem.2014.08.005

Naafs, B. D. A., & Pancost, R. D. (2016). Sea-surface temperature evolution across Aptian oceanic anoxic event 1a. *Geology*, *44*, G38575.1. https://doi.org/10.1130/G38575.1

O'Brien, C. L., Robinson, S. A., Pancost, R. D., Sinninghe, J. S., Schouten, S., Lunt, D. J., et al. (2017). Earth-science reviews Cretaceous sea-surface temperature evolution: Constraints from TEX 86 and planktonic foraminiferal oxygen isotopes. *Earth-Science Reviews*, *172*, 224–247. https://doi.org/10.1016/j.earscirev.2017.07.012

Ohba, M., & Ueda, H. (2010). A GCM study on effects of continental drift on tropical climate at the Early and Late Cretaceous. *Journal of the Meteorological Society of Japan*, *88*(6), 869–881. https://doi.org/10.2151/jmsj.2010-601

Orphan, V. J., House, C. H., Hinrichs, K.-U., McKeegan, K. D., & DeLong, E. F. (2002). Multiple archaeal groups mediate methane oxidation in anoxic cold seep sediments. *Proceedings of the National Academy of Sciences of the United States of America (PNAS)*, *99*, 7663–7668. https://doi.org/10.1073/pnas.072210299

Paillard, D., Labeyrie, L., & Yiou, P. (1996). Macintosh program performs time-series analysis. *Eos, Transactions of the American Geophysical Union*, *77*(39), 379. https://doi.org/10.1029/96EO00259

Pancost, R. D., Sinninghe Damsté, J. S., de Lint, S., van der Maarel, M. J. E. C., Gottschal, J. C., & The Medinaut Shipboard Scientific Party (2000). Biomarker evidence for widespread anaerobic methane oxidation in Mediterranean sediments by a consortium of methanogenic archaea and bacteria. *Applied and Environmental Microbiollogy*, *66*, 1126–1132. https://doi.org/10.1128/AEM.66.3.1126-1132.2000

Pérez-Diaz, L., & Eagles, G. (2014). Constraining South Atlantic growth with seafloor spreading data. *Tectonics*, *33*, 1848–1873. https://doi.org/10.1002/2014TC003644

Pérez-Díaz, L., & Eagles, G. (2017). South Atlantic paleobathymetry since Early Cretaceous. *Scientific Reports*, *7*, 1–16. https://doi.org/10.1038/s41598-017-11959-7

Raynaud, J. F. F., & Robert, P. (1978). Microscopical survey of organic matter from DSDP Sites 361, 362, and 364, in: Deep Sea Drilling Projects and publications; supplement to volumes XXXVIII, XXXIX, XL, and XLI. Pp. 663–669. https://doi.org/10.2973/dsdp.proc.38394041s.306.1978

Repeta, D. J., Simpson, D. J., Jørgensen, B. B., & Jannasch, H. W. (1989). Evidence for anoxygenic photosynthesis from the distribution of bacteriochlorophylls in the Black Sea. *Nature*, *342*(6245), 69–72. https://doi.org/10.1038/342069a0

Rohling, E. J. (1994). Review and new aspects concerning the formation of eastern Mediterranean sapropels. *Marine Geology*, *122*(1-2), 1–28. https://doi.org/10.1016/0025-3227(94)90202-X

Ruble, T. E., Bakel, A. J., & Paul Philp, R. (1994). Compound specific isotopic variability in Uinta Basin native bitumens: Paleoenvironmental implications. *Organic Geochemistry*, *21*(6-7), 661–671. https://doi.org/10.1016/0146-6380(94)90011-6

Rullkötter, J., Mukhopadhyay, P. K., & Welte, D. H. (1984). Geochemistry and petrography of organic matter in sediments from hole 530A, Angola Basin, and hole 532, Walvis ridge, Deep Sea Drilling Project. Cover. Leg 75 cruises drill. Vessel Glomar Chall. Walvis Bay, South Africa, to Recife, Brazil 75, 1069–1087. https://doi.org/10.2973/dsdp.proc.79.132.1984

Schouten, S., Hopmans, E. C., Forster, A., van Breugel, Y., Kuypers, M. M. M., & Sinninghe Damsté, J. S. (2003). Extremely high sea-surface temperatures at low latitudes during the middle Cretaceous as revealed by archeal membrane lipds. *Geology*, *31*(12), 1069–1072. https://doi.org/10.1130/G19876.1

Schouten, S., Van Der Maarel, M. J. E. C., Huber, R., & Damsté, J. S. S. (1997). 2,6,10,15,19-Pentamethylicosenes in *Methanolobus bombayensis*, a marine methanogenic archaeon, and in *Methanosarcina mazei*. *Organic Geochemistry*, *26*, 409–414. https://doi.org/10.1016/S0146-6380(97)00011-9

Schulz, M., & Mudelsee, M. (2002). REDFIT: Estimating red-noise spectra directly from unevenly spaced paleoclimatic time series. *Computers and Geosciences*, *28*(3), 421–426. https://doi.org/10.1016/S0098-3004(01)00044-9

Shipboard Scientific Party (1984). 1. Introduction and explanatory notes, Deep Sea Drilling Project Leg 75 1 Shipboard Scientific Party 2, in: Deep Sea Drilling Project Leg 75; Introduction and Explanatory Notes, Deep Sea Drilling Project Leg 75. pp. 3–25. https://doi.org/10.2973/dsdp.proc.75.101.1984

Sibuet, J., Hay, W. W., Prunier, A., Montadert, L., Hinz, K., & Fritsch, J. (1984). Early evolution of the South Atlantic Ocean: Role of the rifting episode. *The journal of 20th century/contemporary French study*, *75*, 469–481.

Simoneit, B. R. T. (1978). Lipid analyses of sediments from Site 364 in the Angola Basin, DSDP Leg 40, in: S. M. White, P. R. Supko, J. Natland, J. Gardner, J. Herring (Eds.), Initial Reports of the Deep Sea Drilling Project; Supplement to Volumes XXXVIII, XXXIX, XL, and XLI. Texas A & M Univ., Ocean Drilling Program, College Station, TX, United States (pp. 659–662). https://doi.org/10.2973/dsdp.proc.38394041s.305.1978

Sinninghe Damsté, J. S., & de Leeuw, J. W. (1990). Analysis, structure and geochemical significance of organically-bound sulphur in the geosphere: State of the art and future research. *Organic Geochemistry*, *16*(4-6), 1077–1101. https://doi.org/10.1016/0146-6380(90)90145-P

Sinninghe Damsté, J. S., Kuypers, M. M. M., Schouten, S., Schulte, S., & Rullkötter, J. (2003). The lycopane/C31 n-alkane ratio as a proxy to assess palaeoxicity during sediment deposition. *Earth and Planetary Science Letters*, *209*(1-2), 215–226. https://doi.org/10.1016/S0012-821X(03)00066-9

Sinninghe Damsté, J. S., Rijpstra, W. I. C., de Leeuw, J. W., & Schenck, P. A. (1989). The occurrence and identification of series of organic sulphur compounds in oils and sediment extracts: II. Their presence in samples from hypersaline and non-hypersaline palaeoenvironments and possible application as source, palaeoenvironmental and matur. *Geochimica et Cosmochimica Acta*, *53*(6), 1323–1341. https://doi.org/10.1016/0016-7037(89)90066-5

Słowakiewicz, M., Tucker, M. E., Perri, E., & Pancost, R. D. (2015). Nearshore euxinia in the photic zone of an ancient sea. *Palaeogeography Palaeoclimatology Palaeoecology*, *426*, 242–259. https://doi.org/10.1016/j.palaeo.2015.03.022

Stein, R. (1991). Accumulation of organic carbon in marine sediments Springer-Verlag. *Lecture Notes in Earth Sciences*, *34*, 217.
Stein, R., Rullkotter, J., & Welte, D. H. (1986). Accumulation of organic-carbon-rich sediments in the Late Jurassic and Cretaceous Atlantic Ocean—A synthesis. *Chemical Geolology*, *56*(1-2), 1–32. https://doi.org/10.1016/0009-2541(86)90107-5
Stow, D. A. V., & Dean, W. E. (1984). Middle Cretaceous black shales at Site 530 in the southeastern Angola Basin. In *Deep Sea Drilling Projects and publications; part IV: Sedimentology and inorganic geochemistry* (pp. 809–817). Washington, DC: US Government Printing Office. https://doi.org/10.2973/dsdp.proc.75.120.1984
Summons, R. E., Bradley, A. S., Jahnke, L. L., & Waldbauer, J. R. (2006). Steroids, triterpenoids and molecular oxygen. *Philosophical Transactions of the Royal Society B*, *361*(1470), 951–968. https://doi.org/10.1098/rstb.2006.1837
Summons, R. E., Thomas, J., Maxwell, J. R., & Boreham, J. (1992). Secular and environmental constraints on the occurrence of dinosterane in sediments. *Geochimica et Cosmochimica Acta*, *56*(6), 2437–2444. https://doi.org/10.1016/0016-7037(92)90200-3
Summons, R. E., Volkman, J. K., & Boreham, C. J. (1987). Dinosterane and other steroidal hydrocarbons of dinoflagellate origin in sediments and petroleum. *Geochimica et Cosmochimica Acta*, *51*(11), 3075–3082. https://doi.org/10.1016/0016-7037(87)90381-4
Tedeschi, L. R., Jenkyns, H. C., Robinson, S. A., Sanjinés, A. E. S., Viviers, M. C., Quintaes, C. M. S. P., & Vazquez, J. C. (2017). New age constraints on Aptian evaporites and carbonates from the South Atlantic: Implications for oceanic anoxic event 1a. *Geology*, *45*(6), 543–546. https://doi.org/10.1130/G38886.1
van Breugel, Y., Schouten, S., Tsikos, H., Erba, E., Price, G. D., & Damsté, J. S. S. (2007). Synchronous negative carbon isotope shifts in marine and terrestrial biomarkers at the onset of the early Aptian oceanic anoxic event 1a: Evidence for the release of ^{13}C-depleted carbon into the atmosphere. *Paleoceanography*, *22*, PA1210. https://doi.org/10.1029/2006PA001341
Voigt, S., Jung, C., Friedrich, O., Frank, M., Teschner, C., & Hoffmann, J. (2013). Tectonically restricted deep-ocean circulation at the end of the Cretaceous greenhouse. *Earth and Planetary Science Letters*, *369–370*, 169–177. https://doi.org/10.1016/j.epsl.2013.03.019
Volkman, J. K., Barrett, S. M., Dunstan, G. A., & Jeffrey, S. W. (1994). Sterol biomarkers for microalgae from the green algal class Prasinophyceae. *Organic Geochemistry*, *21*(12), 1211–1218. https://doi.org/10.1016/0146-6380(94)90164-3
Volkman, J. K., Kearney, P., & Jeffrey, S. W. (1990). A new source of 4-methyl sterols and 5α(H)-stanols in sediments: Prymnesiophyte microalgae of the genus *Pavlova*. *Organic Geochemistry*, *15*(5), 489–497. https://doi.org/10.1016/0146-6380(90)90094-G
Wagner, T., Hofmann, P., & Flögel, S. (2013). Marine black shale deposition and Hadley cell dynamics: A conceptual framework for the Cretaceous Atlantic Ocean. *Marine and Petroleum Geology*, *43*, 222–238. https://doi.org/10.1016/j.marpetgeo.2013.02.005
Wagner, T., & Pletsch, T. (1999). Tectono-sedimentary controls on Cretaceous black shale deposition along the opening equatorial Atlantic Gateway (ODP Leg 159). *Geological Society of London, Special Publication*, *153*, 241–265. https://doi.org/10.1144/GSL.SP.1999.153.01.15
Wagner, T., Sinninghe Damsté, J. S., Hofmann, P., & Beckmann, B. (2004). Euxinia and primary production in Late Cretaceous eastern equatorial Atlantic surface waters fostered orbitally driven formation of marine black shales. *Paleoceanography*, *19*, PA3009. https://doi.org/10.1029/2003PA000898
Wakeham, S. G., Lewis, C. M., Hopmans, E. C., Schouten, S., & Sinninghe Damsté, J. S. (2003). Archaea mediate anaerobic oxidation of methane in deep euxinic waters of the Black Sea. *Geochimica et Cosmochimica Acta*, *67*(7), 1359–1374. https://doi.org/10.1016/S0016-7037(02)01220-6
Xu, W., Ruhl, M., Jenkyns, H. C., Hesselbo, S. P., Riding, J. B., Selby, D., et al. (2017). Carbon sequestration in an expanded lake system during the Toarcian oceanic anoxic event. *Nature Geoscience*, 10. https://doi.org/10.1038/ngeo2871
Zimmerman, H. B., Boersma, A., & McCoy, F. W. (1987). Carbonaceous sediments and palaeoenvironment of the Cretaceous South Atlantic Ocean. *Geological Society of London, Special Publication*, *26*(1), 271–286. https://doi.org/10.1144/GSL.SP.1987.026.01.19